Coral reef carbonate budgets and ecological drivers in the central Red Sea - a naturally high temperature and high total alkalinity environment

Anna Roik[1,*], Till Röthig[1,+], Claudia Pogoreutz[1], Vincent Saderne[1], Christian R. Voolstra[1]

[1]Red Sea Research Center, King Abdullah University of Science and Technology, 23955 Thuwal, Saudi Arabia

[*]Current address: Marine Microbiology, GEOMAR Helmholtz Centre for Ocean Research, 24105 Kiel, Germany

+Current address: The Swire Institute of Marine Science, Kadoorie Biological Sciences Building, The University of Hong Kong, Pokfulam Road, Hong Kong

Correspondence to: Christian R. Voolstra (christian.voolstra@kaust.edu.sa), Anna Roik (aroik@geomar.de)

Abstract. The structural framework provided by corals is crucial for reef ecosystem function and services, but high seawater temperatures can be detrimental to the calcification capacity of reef-building organisms. The Red Sea is very warm, but total alkalinity is naturally high and beneficial for reef accretion. To date, we know little about how such beneficial and detrimental abiotic factors affect each other and the balance between calcification and erosion on Red Sea coral reefs, that is overall reef growth, in this unique ocean basin. To provide estimates of present-day reef growth dynamics in the central Red Sea, we measured two metrics of reef growth, i.e., *in situ* net-accretion/-erosion rates (G_{net}) determined by deployment of limestone blocks, and ecosystem scale carbonate budgets (G_{budget}) along a cross-shelf gradient (25 km, encompassing near-, mid-, and offshore). Along this gradient, we assessed multiple abiotic (i.e., temperature, salinity, diurnal pH fluctuation, inorganic nutrients, and total alkalinity) and biotic variables (i.e., calcifier and epilithic bioeroder communities). Both reef growth metrics revealed overall congruent patterns from nearshore to offshore: net erosive, neutral, and net accretion states. The average cross-shelf G_{budget} was 0.66 kg m^{-2} y^{-1}, with the highest budget of 2.44 kg m^{-2} y^{-1} measured in the offshore reef. These data are comparable to the contemporary $G_{budgets}$ from the western Atlantic and Indian Ocean, but lie well below "optimal reef production" (5 - 10 kg m^{-2} y^{-1}) and below maxima recently recorded in remote high coral cover reefs sites. Yet, the erosive forces observed in the nearshore reef contributed less as observed elsewhere. A higher total alkalinity accompanied reef growth across the shelf gradient whereas stronger diurnal pH fluctuations were associated with negative budgets. Noteworthy for this oligotrophic region was the positive effect of phosphate, which is a central micronutrient for reef building corals, among others. While parrotfish were substantial contributors to bioerosion, our dataset further highlights coralline algae as important local reef-builders. Altogether, our study establishes a baseline for reef growth in the central Red Sea that will be particularly useful in assessing future trajectories of reef growth capacity under current and future ocean change scenarios.

1 Introduction

Coral reef growth is mostly limited to warm, aragonite-saturated, and oligotrophic tropical oceans and is pivotal for reef ecosystem functioning (Buddemeier, 1997; Kleypas et al., 1999). The coral reef framework not only maintains a remarkable biodiversity, but also provides highly valuable ecosystem services that include food supply and coastal protection, among others (Moberg and Folke, 1999; Reaka-Kudla, 1997). Biogenic calcification, erosion, and dissolution contribute to the formation of the reef framework constructed of calcium carbonate ($CaCO_3$, mainly aragonite). The balance of carbonate loss and accretion is influenced by biotic and abiotic factors. On a reef scale, the main antagonists are calcifying benthic communities, e.g., scleractinian corals and coralline algal crusts, opposed by grazing and endolithic bioeroders, e.g., parrotfish, sea urchins, microbioeroding chlorophytes, boring sponges, and other macroborers (Glynn, 1997; Hutchings, 1986; Perry et al., 2008; Tribollet and Golubic, 2011). The export or loss of carbonate as sediments is considered an essential part, in particular in the wider geomorphic perspective of reef carbonate production states (Cyronak et al., 2013; Perry et al., 2008, 2017). Temperature and carbonate chemistry parameters (e.g., pH, total alkalinity TA, and aragonite saturation state Ω_a, pCO_2) have been identified as important players in regulating these carbonate accretion and erosion processes (Albright et al., 2018; Schönberg et al., 2017). Furthermore, different light regimes across depths, water flow, and wave exposure can alter the rates of reef-formation processes (Dullo et al., 1995; Glynn and Manzello, 2015; Kleypas et al., 2001).

Reef growth is maintained when reef calcification produces more $CaCO_3$ than is being removed, and depends largely on the ability of benthic calcifiers to precipitate calcium carbonate from seawater (e.g., Langdon et al., 2000; Tambutté et al., 2011). TA and Ω_a, positively correlate with calcification rates (Marubini et al., 2008; Schneider and Erez, 2006), and while calcification rates of corals and coralline algae increase with higher temperature, they have upper thermal limits (Jokiel and Coles, 1990; Marshall and Clode, 2004; Vásquez-Elizondo and Enríquez, 2016). Today's ocean is warming and high temperatures begin to exceed the thermal optima of calcifying organisms and thereby slowing down or interrupting calcification (e.g., Carricart-Ganivet et al., 2012; Death et al., 2009). At the same time ocean acidification decreases the ocean's pH and Ω_a (Orr et al., 2005). Arguably, calcification under these conditions could become energetically costlier (Cai et al., 2016; Cohen and Holcomb, 2009; Strahl et al., 2015; Waldbusser et al., 2016). In addition, ocean acidification stimulates destructive processes, for instance the proliferation of bioeroding endolithic organisms (e.g., Enochs, 2015; Fang et al., 2013; Tribollet et al., 2009). Locally impaired reef growth due to an increased intensity or frequency of extreme climate events (Eakin, 2001; Schuhmacher et al., 2005), human impacts including pollution and eutrophication (Chazottes et al., 2002; Edinger et al., 2000), and other ecological events such as population outbreaks of grazing sea urchins or crown-of-thorn starfish that feed on coral can induce reef framework degradation (Bak, 1994; Pisapia et al., 2016; Uthicke et al., 2015). To comparatively assess the persistence of reef framework at regional and global scales, a census-based reef carbonate budget (*ReefBudget*) approach that integrates reef site-specific ecological data into the calculation of the erosion-accretion balance was introduced recently (Kennedy et al., 2013; Perry et al., 2012, 2015). The *ReefBudget* approach shows that 37 % of all current reefs studied are in a net-erosive state (Perry et al., 2013). For the Caribbean, it revealed a 50 % decrease of reef growth compared to historical mid- to late-Holocene reef growth (Perry et al., 2013). Indeed, the use of carbonate

budgets provided valuable insight into the reef growth trajectories in the Seychelles, where surveys conducted since the 1990ies provide important ecological baseline data that were employed in the reef growth calculations (Januchowski-Hartley et al., 2017). Other studies of carbonate budgets highlight the susceptibility of marginal coral reefs to ocean warming and acidification (Couce et al., 2012). Such marginal reefs are found in the Eastern Pacific or in the Middle East in the Persian/Arabian Gulf, where reefs exist at their environmental limits, e.g., low pH or high temperatures, respectively (Bates et al., 2010; Manzello, 2010; Riegl, 2003; Sheppard and Loughland, 2002).

Although the Red Sea features high sea surface temperatures that exceed thermal thresholds of tropical corals elsewhere (Kleypas et al., 1999), it supports a remarkable coral reef framework along its entire coastline (Riegl et al., 2012). Yet, coral skeleton core samples indicate that calcification rates have been declining over the past decades, which has been widely attributed to ocean warming (Cantin et al., 2010). In this regard Red Sea coral reefs are on a similar trajectory as other coral reefs under global ocean warming (Bak et al., 2009; Cooper et al., 2008). In the central and southern Red Sea, present-day data show reduced calcification rates of corals and calcifying crusts when temperatures peaked during summer (Roik et al., 2015; Sawall et al., 2015). While increasing temperatures are seemingly stressful and energetically demanding for reef calcifiers, high TA values, as found in the Red Sea (~ 2400 µmol kg^{-1}, Metzl et al. 1989), are indicative of a putatively beneficial environment for calcification (Albright et al., 2016; Langdon et al., 2000; Tambutté et al., 2011). Little is known about the reef-scale carbonate budgets of Red Sea coral reefs (Jones et al., 2015). Apart from one early assessment of reef growth capacity for a high-latitude reef in the Gulf of Aqaba (northern Red Sea) that considered both calcification and bioerosion/dissolution rates (Dullo et al., 1996), studies only report calcification rates (e.g., Cantin et al., 2010; Heiss, 1995; Roik et al., 2015; Sawall and Al-Sofyani, 2015) or focus on bioerosion generally caused by one group of bioeroders (Alwany et al., 2009; Kleemann, 2001; Mokady et al., 1996). Therefore, we set out to determine reef growth in central Red Sea coral reefs and evaluate the biotic and abiotic drivers. We show and compare two reef growth metrics: G_{net} and G_{budget}. We present net-accretion/-erosion rates (G_{net}) measured *in situ* using limestone blocks deployed in the reefs, which simultaneously capture the rates of epilithic accretion and epilithic and endolithic bioerosion. We also apply a census-based approach adapted from the *ReefBudget* protocol (Perry et al., 2012) to estimate reef growth on an ecosystem scale, as the net carbonate production state or carbonate budget (G_{budget}). To achieve this, we assessed the abundances and calcification rates of major reef-building coral taxa (*Porites*, *Pocillopora*, and *Acropora*) and calcifying crusts (e.g., coralline algae), together with the abundances of epilithic bioeroders (parrotfish and sea urchins) at our study sites. These ecological data were integrated with the Red Sea site- and species-specific calcification or erosion rates to calculate G_{budget}. We then present data from an environmental monitoring of reefs along an environmental cross-shelf gradient during winter and summer. Finally, we correlate potential abiotic and biotic drivers with the two reef growth metrics, G_{net} and G_{budget}. Our study provides a broad and first insight into reef growth dynamics and a comparative baseline to further assess the effects of ongoing environmental change on reef growth in the central Red Sea.

2 Material and Methods

2.1 Study sites and environmental monitoring

Study sites are located in the Saudi Arabian central Red Sea along an environmental cross-shelf gradient, described in detail in Roik et al. (2015) and (2016). Data for this study were collected at four sites: an offshore forereef at ~25 km distance from the coastline (22° 20.456 N, 38° 51.127 E, "Shi'b Nazar"), midshore forereef at ~10 km distance (22° 15.100 N, 38° 57.386 E, "Al Fahal"), and a nearshore forereef (22° 13.974 N, 39° 01.760 E, "Inner Fsar") at ~3 km distance to shore. All sampling stations were located between 7.5 and 9 m depth. In the following, reef sites are referred to as "offshore", "midshore", and "nearshore", respectively. Abiotic variables were measured during "winter" and "summer" 2014. CTD data was collected continuously during "winter" (10th February - 6th April 2014) and "summer" (20th June - 20th September 2014). At each station seawater samples were collected on SCUBA for 5 - 6 consecutive weeks during each of the seasons to determine inorganic nutrients, i.e, nitrate and nitrite (NO_3^-&NO_2^-), ammonia (NH_4^+), phosphate (PO_4^{3-}), and total alkalinity (TA) (Table S1).

2.2 Net-accretion/-erosion rates of limestone blocks

Net-accretion/-erosion rates (G_{net}) were assessed using a "limestone block assay". Blocks cut from "coral stone" limestone were purchased from a local building material supplier in Jeddah, KSA, and each block was fixed with one stainless steel bolt to aluminum racks permanently deployed at the monitoring station of each reef site (a total of 36 blocks, n = 4, Fig. S1). The blocks were oriented in parallel to the reef slope with one side facing up while the other side was facing down towards the reef. Block dimensions were 100 x 100 x 21 mm with an average density of ρ = 2.3 kg L^{-1}. Blocks were dry-weighed before and after deployment on the reefs. Before weighing (Mettler Toledo XS2002S, readability = 10 mg), the blocks were autoclaved and dried in a climate chamber (BINDER, Tuttlingen, Germany) at 40°C for a week. Four replicate blocks were deployed at the reef sites for each exposure timeframe (Fig. 1 a), where they were exposed to the natural processes of calcification and erosion, for 6 months (September 2012 - March 2013), for 12 months (June 2013 - June 2014), and for 30 months each (January 2013-June 2015). All blocks were measured once. Upon recovery, the blocks were treated with 10 % bleach for 24 - 36 h and rinsed with deionized water to remove organic material and any residual salts. G_{net} were expressed as normalized differences of pre-deployment and post-deployment weights [kg m^{-2} y^{-1}] (Table 1).

2.3 Biotic parameters

To assess coral reef benthic calcifier and epilithic bioeroder communities as input data for the reef carbonate budgets, we conducted *in situ* surveys on SCUBA along the cross-shelf gradient at each of our study sites.

2.3.1 Benthic community composition

Community composition and coverage of coral reef calcifying groups were assessed in six replicate transects per site using the belt-transect rugosity method (Perry et al., 2012) as detailed in Roik et al. (2015). From these surveys we extracted data on benthic calcifiers (% cover total hard coral, % hard coral morphs (branching, encrusting, massive, and platy/foliose), % major reef-building coral families (Acroporidae, Pocilloporidae, and Poritidae), % cover calcareous crusts, % recently dead coral, and % rock surface area for carbonate budget calculations (Table S2). In addition, benthic rugosity was assessed in the same transects following the *Chain and Tape Method* (n = 6, Perry et al., 2012).

2.3.2 Epilithic bioeroder/grazer populations along the cross-shelf gradient

For each reef site, we surveyed abundances and size classes of the two main groups of coral reef framework bioerorders, the parrotfishes (Scaridae) (Bellwood, 1995; Bruggemann et al., 1996) and sea urchins (Echinoidea) (Bak, 1994). Surveys were conducted on SCUBA using stationary plots (adapted from Bannerot and Bohnsack, 1986, Text S1) and line transects (n = 6 per site), respectively. Briefly, abundances of parrotfishes and sea urchins were assessed for different size classes. Abundances for all prevalent parrotfish species were assessed in six size classes, based on estimated fork length (FL; FL size classes: 1 = 5 - 14 cm, 2 = 15 - 24 cm, 3 = 25 - 34 cm, 4 = 35 - 44 cm, 5 = 45 - 70, and 6 > 70 cm). We focused on the most abundant bioeroding parrotfish species in the Red Sea (Table S7), which encompassed two herbivorous functional groups: excavators and scrapers (Green and Bellwood 2009). Most abundant across study sites were the excavators *Chlorurus gibbus*, *Scarus ghobban*, and *Cetoscarus bicolor*, and the scrapers *Scarus frenatus*, *Chlorurus sordidus*, *Scarus niger* and *Scarus ferrugenius*, as described in Alwany et al., 2009. Additionally, we counted *Hipposcarus* harid, which occurred frequently at the study sites, along with members of the genus *Scarus* that could not be identified to species level and were therefore pooled in the category of 'Other *Scarus*'. Both *H. harid* and *Scarus* spp. were broadly categorized as scrapers (Green and Bellwood, 2009). The sea urchin census targeted five size classes of the four most common bioerosive genera *Diadema*, *Echinometra*, *Echinostrephus*, and *Eucidaris*, based on urchin diameter (size classes 1 = 0 - 20 mm, 2 = 21 - 40 mm, 3 = 41 - 60 mm, 4 = 61 - 80 mm, 5 = 81 - 100 mm). For details on the field surveys and data treatment for biomass conversion, refer to the supplementary materials (Text S1 and references therein).

2.4 Reef carbonate budgets

Ecosystem scale reef carbonate budgets, G_{budget} [kg m^{-1} y^{-1}], were determined following the census-based *ReefBudget* approach by Perry et al. (2012) (Table 1). G_{budget} incorporates local census data, site-specific net-accretion/-erosion data (G_{net} over 30 months) and calcification data (buoyant weight measurements) collected for the present and from a previous study (Roik et al., 2015). Importantly, the approach incorporates epilithic bioerosion, which is based on abundance rather than assessment of actual bite or erosion rates; therefore, parrotfish and sea urchin census data collected in this study are readily employed in the *ReefBudget* calculations using bite and erosion rates from the

literature (Alwany et al., 2009; Perry et al., 2012). In summary, site-specific benthic calcification rates ($G_{benthos}$, kg m^{-1} y^{-1}), net-accretion/-erosion rates of reef "rock" surface area ($G_{netbenthos}$, kg m^{-1} y^{-1}), and epilithic erosion rates by sea urchins (E_{echino}, kg m^{-1} y^{-1}) and parrotfishes (E_{parrot} , kg m^{-1} y^{-1}), were determined for the G_{budget} calculations (Fig. 1 (b) and Fig. 3 (a)). A detailed account of Red Sea specific calculations and modifications of the *ReefBudget* approach employed in this study are outlined in the supplementary materials (Text S1, Equation box S1-3, and Tables S2-7).

2.5 Abiotic parameters

2.5.1 Continuous data: temperature, salinity, and diurnal pH variation

Factory-calibrated "conductivity-temperature-depth" loggers (CTDs, SBE 16plusV2 SEACAT, RS-232, Sea-Bird Electronics, Bellevue, WA, USA) were deployed at the monitoring stations 0.5 m above the reef to collect time series data of temperature, salinity, and pH_{NBS} at hourly intervals. The pH probe (SBE 18/27, Sea-bird Electronics) was factory calibrated and verified using NBS scale standard buffers (pH 7 and 10, Fixanal, Fluka Analytics, Sigma Aldrich, Germany).

2.5.2. Seawater samples: Inorganic nutrients and total alkalinity

Seawater samples were collected on SCUBA at each of the stations using 4 L collection containers (Table S1). Simultaneously, 60 mL seawater samples were taken through a 0.45 µm syringe filter for TA measurements. Seawater samples for inorganic nutrient analyses and TA measurement were transported on ice in the dark and were processed on the same day. Samples were filtered over GF/F filters (0.7 µm, Whatman, UK) and filtrates were frozen at -20°C until analysis. The inorganic nutrient content (NO_3^-&NO_2^-, NH_4^+, and PO_4^{3-}) was determined using standard colorimetric tests and a Quick-Chem 8000 AutoAnalyzer (Zellweger Analysis, Inc.). TA samples were analyzed within 2 - 4 h after collection using an automated acidimetric titration system (Titrando 888, Metrohm AG, Switzerland). Gran-type titrations were performed with a 0.01 M HCl (prepared from 0.1 HCl Standard, Fluka Analytics) at an average accuracy of ± 9 µmol kg^{-1} (SD of triplicate measurements).

2.6 Statistical analyses

2.6.1 Net-accretion/-erosion rates and carbonate budgets

G_{net} data (Table 2) were tested for effects of the factors "reef" (fixed factor: nearshore, midshore, and offshore) and "deployment time" (random factor: 6, 12, and 30 months). A univariate 2-factorial PERMANOVA was performed on $\log_n(x+1-\min(x_{1-n}))$ transformed data using Euclidian distance matrix 9999 permutations of residuals under a reduced model and type III partial sum of squares. Pair-wise tests followed where applicable (PRIMER-E V6, Table S9).

G_{budget} data (Table 3) were tested for statistical differences between the reef sites (fixed factor: nearshore, midshore, and offshore) using a 1-factorial ANOVA. In parallel, $G_{benthos}$ was tested using a 1-factorial ANOVA with $\log_{10}$ transformed data, while non-parametric Kruskal-Wallis tests were employed for non-transformed $G_{netbenthos}$, E_{echino}, and E_{parrot} data. Tukey's HSD post-hoc tests or Dunn's multiple comparisons followed where applicable (Table S10).

Assumptions were evaluated by histograms and the Shaphiro-Wilk normality test. Statistical tests were performed as implemented in R environment (R Core Team, 2013). Bar plots were generated using *ggplot2* in R (Fig 2 and 3).

2.6.2 Abiotic parameters

All abiotic data were summarized as means, standard deviations per reef and season and over each season (Table 4) and boxplots were generated (Fig. 4). Diurnal pH variation was extracted from the continuous data as the pH_{NBS} standard deviation per day. Outliers were detected and removed from the TA data. All outliers (data points beyond the upper boxplot 1.5 IQR) clustered to one sampling day (23 June 2014), therefore likely an artifact of the chemical analysis. All continuous abiotic variables and inorganic nutrients (PO_4^{3-} after square-root transformation) fulfilled parametric assumptions and were evaluated using univariate 2-factorial ANOVAs testing the factors "reef" (nearshore, midshore, and offshore) and "season" (winter and summer). TA data was square-root transformed, which improved symmetry of data (Anderson et al., 2008), and tested under the same 2-factorial design, as outlined above, using a PERMANOVA (Euclidian resemblance matrix and 9999 permutations of residuals under a reduced model and type II partial sums of squares). Within each significant factor Tukey's HSD post-hoc tests or PERMANOVA integrated pair-wise tests followed (Table S11 and S12). Assumptions were evaluated by histograms and the Shaphiro-Wilk normality test. Statistical tests and outlier detection were performed in R environment or PRIMER-E V6. Boxplots were generated using *ggplot2* in R (Fig. 4).

2.6.3 Abiotic-biotic correlations

To evaluate the relationship of abiotic and biotic predictors of G_{net} and G_{budget}, Spearman rank correlation coefficients were obtained for the predictor variables (at a confidence level of 95%) using *cor.test* in R (R Core Team, 2013; Wickham and Chang, 2015). *P*-values were adjusted using *p.adjust* in R employing the Benjamini-Hochberg method. Correlations were performed using G_{net} data obtained in the 30-months measurements from the reef sites (nearshore, midshore, and offshore) (Table 5 and Table S13). Predictor variables were the site-specific means of CTD measured variables (temperature, salinity, and diurnal pH variation), means of inorganic nutrients (NO_3^-&NO_2^-, NH_4^+, and PO_4^{3-}), and total alkalinity (TA), see Table 4. Biotic predictors were variables that likely impacted the limestone blocks, i.e. parrotfish abundances, sea urchin abundances, calcareous crusts cover, and algal and sponge cover. Since we did not observe any coral recruits on the blocks, we did not include % coral cover and related variables in the correlations. G_{budget} correlations included all the above-mentioned abiotic variables and 13 biotic transect variables (i.e., parrot fish abundances, sea urchin abundances, % branching coral, % encrusting coral, % massive coral, % platy/foliose coral, % of Acroporidae, % Pocilloporidae, % Poritidae, % total hard coral cover, calcareous crusts cover, algal and sponge cover, and rugosity). Prior to analysis, some of the predictors (i.e., % platy/foliose corals and % Poritidae) were $\log_{10}(x+1)$ transformed to improve the symmetry in their distributions (Table 5 and Table S14).

3 Results

3.1 Net-accretion/-erosion rates of limestone blocks

Net-accretion/-erosion rates G_{net} were measured in assays over periods of 6, 12, and 30 months in the reef sites along the cross-shelf gradient. These measurements represent the result of calcification and bioerosion processes impacting the deployed blocks. Visible traces of boring endolithic fauna were only found on the surfaces of blocks recovered after 12 and 30 months as presented in Fig. 2 (c)-(f). A brief visual inspection of the block surfaces after retrieval showed colonization by coralline algae, bryozoans, boring sponges, small size boring worms and clams, as well as parrotfish bite-marks. No coral recruits were identified. Further analyses of the established calcifying and bioeroding communities were not within the scope of this study. G_{net} based on the 30-months deployment of blocks ranged between -0.96 and 0.37 kg m^{-2} y^{-1} (Table 2). G_{net} for 12 and 30-months blocks were negative on the nearshore reef (between -0.96 and -0.6 kg m^{-2} y^{-1}, i.e., net erosion is apparent), slightly positive on the midshore reef (0.01 - 0.06 kg m^{-2} y^{-1}, i.e., almost neutral carbonate production state), and positive on the offshore reef (up to 0.37 kg m^{-2} y^{-1}, i.e., net accretion of reef framework). Deployment times had a significant effect on the variability of G_{net} (Pseudo-F = 5.9, $p_{PERMANOVA}$ < 0.01, Table S9). As expected, accretion/erosion was overall higher when measured over the longer deployment period (Fig. 2 (g)) in comparison to the shorter deployment times, reflecting the continuous and exponential nature of bioerosion due to the colonization progress of fouling organisms over time. The significant interaction of reef site and deployment time (Pseudo-F = 7.3, $p_{PERMANOVA}$ < 0.001) shows that only blocks deployed over 12 and 30 months revealed significant site variability, specifically the differences between nearshore vs. offshore and midshore vs. offshore sites became evident ($p_{pair\text{-}wise}$ < 0.05, Table S9). The within-group variability was highest for the nearshore reef, where standard deviations were up to 7-times higher compared to the midshore and the offshore reefs.

3.2 Biotic parameters

3.2.1 Benthic community composition

A detailed account of benthic community structure of the study sites is provided in Roik et al. (2015). In brief, a low percentage of live substrate (20 %) and calcifier community cover (hard corals = 11 % and calcifying crusts = 1 %) was characteristic at the nearshore site, while rock (23 %) and rubble (4 %) were more abundant compared to the other sites. The midshore and offshore reefs provided live benthos cover of around 70 % and a large proportion of calcifiers (48 and 59 %). The proportion of coral and calcifying crusts, which were dominated by coralline algae, were 38 % and 10 % in the midshore compared to 35 % and 23 % in the offshore reef, respectively. Major reef-building coral families were Acroporidae, Pocilloporidae, and Poritidae forming 32 - 56 % of the total hard coral cover. A soft coral community (of around 25 %) occupied large areas in the midshore reef. This community was minor in the nearshore and offshore reefs with 4 % and 8.5 %, respectively. Specific benthic accretion rates $G_{benthos}$ [kg m^{-2} y^{-1}], which were used as input data for the G_{budget} calculation, were constructed using these benthic data in addition to site and calcifier specific calcification rates (Tables S2-3).

3.2.2 Epilithic bioeroder/grazer populations along the cross-shelf gradient

A total of 718 parrotfishes and 110 sea urchins were observed and included subsequent *ReefBudget* analyses. Parrotfish mean abundances and biomass estimates ranged between 0.08 ± 0.01 and 0.17 ± 0.60 individuals m^{-2}, and 24.69 ± 6.04 and 82.18 ± 46.67 g m^{-2}, respectively (Table S6). The largest parrotfishes (category 5 parrotfish, i.e., > 45 - 69 cm fork length) were observed at the midshore site. With the exception of the midshore reef, category 1 (5 - 14 cm) parrotfish were commonly observed at all sites. Large parrotfishes (category 6 with ≥ 70 cm fork length) were not observed during the surveys. For sea urchins, mean abundances of 0.002 ± 0.004 - 0.014 ± 0.006 individuals m^{-2} per site were observed and mean biomasses 0.05 ± 0.04 - 1.43 ± 0.98 g m^{-2} estimated per site, respectively (Table S4). The midshore site exhibited the largest range of sea urchin size classes (from categories 1 or 2 to the largest size class 5), while at the other two exposed sites, only the two smallest size classes of sea urchins were recorded.

3.3 Reef carbonate budgets

The carbonate budget, G_{budget}, averaged over all sites was 0.66 ± 2.01 kg m^{-2} y^{-1} encompassing values ranging from a negative nearshore budget (-1.48 ± 1.75 kg m^{-2} y^{-1}) to a positive offshore budget (2.44 ± 1.03 kg m^{-2} y^{-1}) (Figure 3 and Table 3). G_{budget} significantly differed between reef sites ($F = 16.7$, $p_{ANOVA} < 0.001$, Table S10), where nearshore vs. offshore site and midshore vs. offshore site showed significant differences ($p_{Tukey\ HSD} < 0.01$). Further, biotic variables that contribute to the final G_{budget} were heterogeneous: $G_{benthos}$ significantly varied between midshore vs. nearshore site and offshore vs. nearshore site ($p_{Tukey\ HSD} < 0.01$), $G_{netbenthos}$ varied between all site combinations ($p_{Tukey\ HSD} < 0.001$), E_{echino} significantly differed between midshore and nearshore, and E_{parrot} variability was similar at all sites. The within-group variations for the nearshore reef was 5-times higher compared to the midshore reef and the offshore reef ranged in between. Overall, the proportional loss of accreted carbonate to bioerosion was 15 % in the offshore reef, 42 % in the midshore reef, and over 100 % in the nearshore reef, where bioerosion was 4-fold higher than accretion.

3.4 Abiotic parameters

3.4.1 Temperature, salinity, and diurnal pH variation

We used abiotic monitoring data to characterize environmental conditions at each reef site throughout the year (Table 1, Table S10 and S12). Temperature and salinity included around 4400 data points per reef site in the nearshore and offshore reef, and ~2700 in the midshore reef; diurnal pH SDs were 185 data points for the midshore and offshore site, and 87 for the nearshore site. The seasonal mean temperature varied between 26.1 ± 0.5°C in winter and 30.9 ± 0.7°C in summer across all reefs. The cross-shelf difference was largest in summer (~0.6°C), and significant during both seasons ($F = 1042.6$, $p_{ANOVA} < 0.001$). From all sites, the nearshore site experienced the lowest mean temperature (26.1°C) in winter and the highest (31.3°C) in summer. During summer 30.6 - 30.7°C were recorded at the midshore

and offshore reefs. Overall salinity was high ranging between 39.18 – 39.44 ppt over the year. In summer nearshore salinity was significantly increased by 0.36 ppt compared to winter and by 0.18 ppt higher compared to the other reefs (F = 945.3, p_{ANOVA} < 0.001). Salinity in the midshore and offshore reef was not significantly different. Mean diurnal standard deviations of pH ranged between 0.04 – 0.07 SD of pH units in the midshore and offshore reefs. The nearshore reef experienced the largest diurnal variations that result in a mean of 0.29 SD during winter and 0.6 SD of pH units during summer. The diurnal pH fluctuation differed significantly between all reef sites (F = 1241.47, p_{ANOVA} < 0.001).

3.4.2 Seawater samples: Inorganic nutrients and total alkalinity

Concentrations of all measured inorganic nutrients were below 1 µmol kg^{-1} (Table 1). NO_3^-&NO_2^- was on average between 0.63 ± 0.26 and 0.28 ± 0.22 µmol kg^{-1}, NH_4^+ between 0.51 ± 0.17 and 0.35 ± 0.19 µmol kg^{-1}, and PO_4^{3-} as low as 0.02 ± 0.01 and 0.09 ± 0.02 µmol kg^{-1} (the highest and lowest site-season averages are reported here). By trend mean NO_3^-&NO_2^- and NH_4^+ levels were higher in winter compared to summer comprising a difference of 0.29 and 0.16 µmol kg^{-1}, respectively (Fig. 4, Table S11 and S12). In contrast, PO_4^{3-} was significantly higher in winter than in summer with means differing on average by 0.04 µmol kg^{-1} (F = 16.0, p_{ANOVA} < 0.001, Table S11). Mean differences across the shelf were 0.1µmol kg^{-1} in NO_3^-&NO_2^- during winter, 0.1 µmol kg^{-1} in NH_4^+ during summer, and 0.02 µmol kg^{-1} in PO_4^{3-} throughout both seasons.

Total alkalinity (TA) ranged between 2391 ± 15 and 2494 ± 16 µmol kg^{-1}. TA was significantly different between seasons and reef sites (Pseudo-F_{season} = 297.6, Pseudo-$F_{reefsite}$ = 22.5, $p_{PERMANOVA}$ < 0.001, Table S11 and S12). During both seasons TA was decreasing from offshore to the nearshore reef. During winter, TA was slightly higher with 2487 ± 20 µmol kg^{-1} compared to 2417 ± 27 µmol kg^{-1} in summer. The increase from nearshore to offshore was on average between 20 and 50 µmol kg^{-1} (Fig. 4).

3.5 Abiotic-biotic correlations

Strong and positive G_{net}-correlates were calcareous crust cover, NO_3^-&NO_2^-, PO_4^{3-}, and TA. Negative correlates were salinity, diurnal pH variation, and parrotfish abundance (strong correlates: $\rho > |0.75|$, $p < 0.001$). Abiotic G_{budget}-correlates were exactly the same set of variables as for G_{net}. Biotic correlates of G_{budget} were only positive relationships, including calcareous crusts, hard corals, and rugosity. Parrotfish and sea urchin abundances had a negative effect on G_{budget}. However, the correlation was weak and not significant ($\rho \sim -0.5$). The non-calcifying benthos, which represents the coverage by algae, soft corals, and sponges, was not correlated with the dynamics of G_{budget} and was correlated only weakly and not significantly with G_{net} ($\rho \sim 0.5$) (Table 5, Table S13 and S14).

4 Discussion

Central Red Sea reefs are dominantly governed by unique environmental conditions of high temperature, salinity, total alkalinity, and oligotrophy (Fahmy, 2003; Kleypas et al., 1999; Steiner et al., 2014). On a global scale they support remarkable reef growth, supporting well established fringing reefs along most of the coast. To date, processes contributing to reef growth in various regions of the Red Sea have mostly been investigated individually. For instance, some studies focused on bioerosion by one specific group of bioeroders only (Alwany et al., 2009; Kleemann, 2001; Mokady et al., 1996), while other studies assessed calcification of reef-building corals (e.g., Cantin et al., 2010; Heiss, 1995; Roik et al., 2015; Sawall et al., 2015). Hence, the present study aimed for a detailed picture of reef growth in the central Red Sea by integrating the antagonistic processes of calcification and bioerosion. This we achieved in a two-step process assessing two central metrics of reef growth along a cross-shelf gradient. First, we assessed net-accretion and net-erosion rates (G_{net}) from three reef sites along the cross-shelf gradient *in situ* using a limestone block assay. Second, we constructed ecosystem-scale estimates of reef carbonate budgets for Red Sea reef sites (G_{budget}) adapting the census-based ReefBudget approach by Perry et al. (2012). Discussing our data, we highlight the difficulties understanding dynamics and interactions of reef growth processes in their multivariate environmental setting. We further discuss the importance of carbonate budgets as a powerful tool to explore the trajectories of reef growth in a global and historical context.

4.1 Net accretion/erosion rates (G_{net}) in the central Red Sea

4.1.1 Cross-shelf dynamics in a global context

The limestone block assay revealed three reef production states in the central Red Sea: 1) net erosion (nearshore), 2) near-neutrality (midshore), and 3) net accretion (offshore). These nearshore to offshore spatial patterns observed in our study region represent a common cross-shelf reef pattern. This is in contrast to the pattern observed on the Great barrier reef (GBR), where total bioerosion rates were higher in offshore reefs than inshore driving net-erosion (Tribollet et al., 2002; Tribollet and Golubic, 2005). Generally, most block assay studies conducted in various reef habitats and regions mostly delivered net-erosive rates. In the Red Sea net erosion was only observed nearshore (-0.96 kg m^{-2} yr^{-1}, 30 months deployment), which is moderate compared to erosion rates measured in the GBR, French Polynesia, and Thailand (-4 or -8 kg m^{-2} yr^{-1}) (Osorno et al., 2005; Pari et al., 1998; Schmidt and Richter, 2013; Tribollet and Golubic, 2005). The midshore reef was characterized by near-neutral, i.e., minor net accretion (0.06 kg m^{-2} yr^{-1}). Comparable net accretion rates (0.08 and 0.62 kg m^{-2} yr^{-1}) were previously recorded in French Polynesia, however only based on few reef sites of uninhabited atolls (Pari et al., 1998).

Our limestone block assays captured a substantial net-accretion rate on a small scale, in particular for the offshore reef site in the central Red Sea (0.37 kg m^{-2} yr^{-1} net accretion). Similarly, studies from reefs in Southeast Asia, e.g., at the coasts of the Thai Andaman Sea and Indonesian Java Sea, note that the accretion by calcifying crusts, such as coralline algae, were negligible compared to the high degree of bioerosion measured in the limestone blocks (Edinger et al., 2000; Schmidt and Richter, 2013).

4.1.2 Limestone block deployment time and biotic drivers

Our data show that G_{net} values were overall highest with longer deployment times, reflecting the succession and early establishment of calcifying crust and bioeroding communities on the limestone blocks. Due to our sampling design (weight-based block assay), accretion and erosion processes however are simultaneously captured and cannot be disentangled. Overall, the block assay data are indicative of a calcifier-friendly offshore environment and a nearshore reef habitat increasingly supporting endolithic bioeroders.

According to the literature, the carbonate loss in the 12-month blocks from the nearshore site was partly due to a young microbioeroder community, which is typically most active during this early phase. During the early stages of colonization by endolithic microorganisms, the chlorophyte *Ostreobium sp*. predominantly contributes to microbioerosion, while the erosion rate steadily increases with deployment time (Grange et al., 2015; Tribollet and Golubic, 2011). Microbioerosion rates have been reported to be -0.93 kg m^{-2} yr^{-1} after 12 months of block exposure, which represents the average rate, at the early colonization stage when the steadily increasing microbioerosion rate has leveled off (Grange et al., 2015). This rate is slightly higher compared to our measurements of net erosion in the nearshore site after the same deployment time (i.e, -0.61 kg m^{-2} yr^{-1}), and the difference may reflect measurements encompassing both, bioerosion and accretion.

Previously, studies have shown that site differences in total bioerosion became typically visible after 1 year of deployment and were significantly enhanced after 3 years (Tribollet and Golubic, 2005). The deployment time of 12 months in our study accordingly was sufficient to reveal a difference between our most distant sites, i.e., nearshore and offshore reef. Further, calcifying crusts, specifically coralline algae, observed on all blocks from the offshore reef contributed to the respective net accretion. This is corroborated by the positive correlation of their abundances with G_{net} across all reef sites. In this study we can exclude the contribution of coral recruits, as corals have not successfully settled on any limestone block.

Significant differences in accretion/erosion between all three sites of the cross-shelf gradient became apparent after 30 months deployment, and macroborer traces were observed in blocks for the first time (Fig. 2). Over the course of 2 - 3 years, macrobioeroders such as polychaetes, sipunculids, bivalves, and boring sponges can establish communities in limestone blocks (Hutchings, 1986). Between the first two years, macrobioeroder contribution to the total bioerosion can quadruple (0.02 - 0.09 kg m^{-2} yr^{-1}), before levelling off around 3-4 years post-deployment (Chazottes et al., 1995). In our study, the increase of G_{net} between the 12- and 30-month deployment (~0.30 kg m^{-2} yr^{-1} on average in the nearshore and offshore site) indicates that calcifying and eroding communities were still in a state of succession. We cannot rule out that the blocks deployed for 30 months still represent an immature community and underestimate maximal calcification and erosion rates.

Correlation analyses indicate a significant contribution of parrotfish to the net erosion rates in the nearshore reef. This observation is in line with previous work demonstrating a significant contribution of parrotfish activity to bioerosion (Alwany et al., 2009; Bellwood, 1995; Bellwood et al., 2003). By comparison, sea urchin size and abundance do not appear to be significant for bioerosion on the studied central Red Sea reefs. On other reefs, sea urchin bioerosion can be substantial, equaling or even exceeding reef carbonate production (Bak, 1994). The low contribution of sea urchins to bioerosion on central Red Sea reefs may be a result of potentially low abundances of highly erosive sea urchins

(McClanahan and Shafir, 1990). The correlation results support observed parrotfish bite-marks and a lack of sea urchins on and in the direct vicinity of the recovered blocks. Taken together, our data and the existing literature suggest that endolithic micro- and macrobioerosion, as well as by parrotfish feeding likely contributed substantially to the carbonate loss.

4.2 Carbonate budgets (G_{budget}) in the central Red Sea

4.2.1 Cross-shelf dynamics, regional and global context

On an ecosystem scale, G_{budget} dataset suggest that the offshore site in the central Red Sea loses about 15 % accreted carbonates a year to bioerosion. On the mid- and nearshore reef, this loss is equal to 42 % and to over 100 %, respectively. By comparison - on the scale of a single coral colony, the boring clam *Lithophaga lessepsiana* alone can erode up to 40 % of the carbonate deposited by the coral *Stylophora pistillata* (Lazar and Loya, 1991). In our study sites, the spatial dynamics of the two metrics, G_{net} and the census-based G_{budget}, were congruent, i.e., suggestive of a net-eroding reef in the nearshore site, and a growing reef in the offshore site. This observation indicates that the balance of accretion and erosion can be very similar at a small and large scale.

Reef growth at the central Red Sea cross-shelf gradient averaged 0.66 ± 2.01 kg m^{-2} y^{-1}, which was driven by the offshore reef, reflecting the location and habitat dependence for reef growth potential. A similar scenario has been observed on a reef platform in the Maldives, where heterogeneous reef accretion occurs and small reef areas can promote substantial net accretion and thereby greatly contribute to the maintenance of reef scale overall positive budgets (Perry et al., 2017).

The here presented central Red Sea G_{budget} data are well within the range of contemporary reef carbonate budgets in the tropical western Atlantic (2.55 ± 3.83 kg m^{-2} y^{-1}) and the Indian Ocean (1.41 ± 3.02 kg m^{-2} y^{-1}) (Perry et al., 2018). However, our data along with most contemporary budgets are well below the suggested "optimal reef budget" of 5 - 10 kg m^{-2} y^{-1} observed in "healthy", high coral cover fore-reefs in both geographic regions (Perry et al., 2018; Vecsei, 2004). This coincides with the observed decrease in calcification rates of Red Sea corals due to the global warming trend (Cantin et al., 2010), which might have severe implications for contemporary and future reef formation in the region at large. While the present G_{budget} data strongly suggest effective barrier reef formation in the central Red Sea (substantial accretion on the offshore reef), carbonate accretion rates and therefore reef formation in the central Red Sea may be hampered in the long run by the ongoing warming.

4.2.2 Biotic drivers

Regional differences

Cross-shelf patterns of G_{budget} drivers from the central Red Sea including variables of accretion and erosion were distinct from other reef systems. Specifically, the central Red Sea system is characterized by a protected nearshore site, which supported a negative G_{budget} impacted by high parrotfish abundances and erosion rates, low coral cover, and assumedly considerable endolithic bioerosion rates (see discussion of G_{net} data). In contrast, the offshore reef was

458 characterized by high calcification rates, driven by high coral and coralline algae abundances. In the GBR an opposing
459 trend with high net accretion in the nearshore reefs (Browne et al., 2013) coincided with high coral cover, low bierosion
460 rates, and lowest rates of parrotfish bioerosion (Hoey and Bellwood, 2007; Tribollet et al., 2002). On Caribbean reefs,
461 parrotfish erosion rates were higher on leeward reefs (which may be similar to protected nearshore habitats), but in
462 contrast to the central Red Sea, these sites were typically characterized by overall high coral cover driving a positive
463 G_{budget} (Perry et al., 2012, 2014). This inter-regional comparison strongly suggests that reef accretion/erosion dynamics
464 encountered in any given reef system cannot be readily extrapolated to other reef systems. Hence, *in situ* assessments
465 of individual reef systems are required to unravel local dynamics and responses to environmental change, and therefore
466 imperative for the development of effective management measures.
467
468 *The role of coral and coralline crusts*
469 Benthic calcifiers, in particular reef-building corals, are major contributors to carbonate production and are considered
470 the most influential drivers of $G_{budgets}$ globally (Franco et al., 2016). Corals in particular can contribute as much as 90
471 % to the gross carbonate production across different reef zones, which also includes low coral cover lagoonal and
472 rubble habitats (Perry et al., 2017). Hence, the loss of coral cover rapidly gives way to increased bioerosion, and is
473 thereby a critical force of degradation of the reef framework (Perry and Morgan, 2017). Indeed, on Caribbean reefs,
474 G_{budget} data were reported to shift into erosional states once live hard coral cover was below 10 % (Perry et al., 2013).
475 A live coral cover threshold remains to be determined for the central Red Sea and will require evaluation of a larger
476 dataset. Yet, we find that the nearshore reef featuring a negative G_{budget} is characterized by a coral cover of 11 %, while
477 the midshore and offshore reefs, characterized by near-neutral vs. positive carbonate budgets, both feature similar
478 average coral cover (35 and 40 %, respectively). In this respect, our data show that a 2-fold higher abundance of
479 coralline algae and other encrusting calcifiers in the offshore reef (compared to the midshore reef) significantly added
480 to a higher G_{budget}. The positive contribution of coralline algae for central Red Sea reef accretion is corroborated by
481 their strong and significant correlation to G_{budget}. Coralline algae in particular are considered an important driving
482 force of reef growth, as they stabilize the reef framework through "cementation" (Perry et al., 2008) and by habitat
483 priming for successful coral recruitment (Heyward and Negri, 1999).
484
485 *Epilithic grazers*
486 Epilithic grazers such as parrot fish and sea urchin are considered important drivers of bioerosion on many reefs (Hoey
487 and Bellwood, 2007; Mokady et al., 1996; Pari et al., 1998; Reaka-Kudla et al., 1996). Sea urchins were identified as
488 significant bioeroders in some reefs of Reunion Island, French Polynesia, and in the Gulf of Aqaba, northern Red Sea
489 (Chazottes et al., 1995, 2002; Mokady et al., 1996). At the latter, sea urchins were abundant, and their removal of reef
490 carbonates was estimated to range around 13 - 22 % of total reef slope calcification (Mokady et al., 1996). In contrast,
491 sea urchins were rare in our study sites contributing to only 2 - 3 % of the total bioerosion resulting in low contributions
492 to G_{budget}. Only on the net-erosive nearshore reef sea urchins were more abundant causing 12 % of total bioerosion.
493 Compared to sea urchins, parrotfish played a more important role for $G_{budgets}$ throughout the entire reef system,
494 contributing 70 - 96 % of the total bioerosion. In the correlation analyses, both grazers, i.e., sea urchins and parrotfish,

negatively correlated with G_{budget}, however these correlations were not very strong ($\rho \sim -0.5$) and non-significant. The weak correlation may be influenced by a considerable variability in the reef census dataset, specifically regarding parrotfish abundances. Observer bias (parrotfish keep minimum distance from surveyors during dives and may therefore not enter survey plots; pers. obs.), natural (e.g., species distribution, habitat preferences, reef rugosity, and mobility or large roving excavating species, such as *Bolbometopon muricatum*), and/or anthropogenically-driven factors (e.g., differential fishing pressure) may also contribute to the observed data heterogeneity (McClanahan, 1994; McClanahan et al., 1994). Indeed, the Saudi Arabian central Red Sea has been subject to decade-long unregulated fishing pressure, which has significantly altered reef fish community structures and reduced overall fish biomass compared to less impacted Red Sea regions (Kattan et al., 2017). Unregulated fishing could at least in part explain the differences of fish abundance dynamics between the present study and reefs on the GBR and the Caribbean. The heterogeneity of grazer populations further propagates into $G_{budgets}$ estimates, resulting in a considerable within-site variability that reduces power of statistical tests and correlations.

The presented data indicates parrotfish as the main contributors to a negative nearshore G_{budget}, which could characterize these grazers as a threat to the reef framework stability on reefs with low carbonate accretion potential. However, careful interpretation requires to consider the ecological role of parrotfish. While low parrotfish abundances may directly reduce reef erosion pressure, lowered grazing rates can promote phase-shifts to non-calcifying organisms, such as fleshy macroalgae (Hughes et al., 2007; Mumby, 2009). Parrotfish feeding regulates benthic algal growth, which in turn supports the recruitment of reef calcifiers such as corals, ultimately helping maintain a coral-dominated state. Indeed, removal of algal turfs by parrotfish affects coral reefs down to microbial scales (e.g., reduction of putative pathogens, Zaneveld et al., 2016). Finally, overfishing of (parrot)fishes can reduce feeding pressure on bioeroders or their larvae (e.g., sea urchins), resulting in an uncontrolled population increase leading reefs on a trajectory of degradation (Edgar et al., 2010; McClanahan and Shafir, 1990). Therefore, well managed fish stocks have a positive effect on the long-term maintenance of carbonate budgets and the recovery potential of a reef (Mumby and Harborne, 2010).

4.3 Abiotic factors and reef growth dynamics

Reef habitats in the central Red Sea are characterized by abiotic factors that differ from the majority of tropical reef environments (Couce et al., 2012; Kleypas et al., 1999). Our sites were exposed to high summer temperatures (30 - 33 °C) and a high salinity throughout the year (39 - 40 ppt). Inorganic nutrients were mostly far below 1 µmol kg^{-1}, whereas total alkalinity (TA) was comparably high, 2400 – 2500 µmol kg^{-1}, values typical for much of the Red Sea basin (Acker et al., 2008; Steiner et al., 2014). As such, the Red Sea is considered a natural model system or "laboratory", which can advance our understanding of ecosystem functioning under extreme or marginal conditions of which some are projected under ocean change scenarios (Camp et al., 2018). The study of such natural systems is a challenge and the documentation of governing factors both abiotic and biotic will be paramount to a better understanding of the dynamics and interactions, which can significantly improve ecosystem scale predictions (Boyd and Hutchins, 2012; Boyd and Brown, 2015; Camp et al., 2018).

In the present study, reef framework decline (i.e., net erosion) was associated with the reef habitat of slightly increased salinity and stronger diel pH fluctuations, which are characteristic for shallow water, limited flow systems and semi-enclosed reefs (Camp et al., 2017; Shamberger et al., 2017), such as the here investigated nearshore study site (Roik et al., 2016). On the other hand, positive reef growth was associated with reef habitats characterized by comparably higher TA levels, but also with slightly increased inorganic nutrient species, namely NO^{3-}&NO^{2-} and PO_4^{3-}. The outcomes of correlations between abiotic data and both reef growth metrics G_{net} and G_{budget} overlap, because of common cross-shelf dynamics.

The nearshore site

The nearshore reef is located on the shelf, surrounded by shallow waters of extended residency time (Roik et al., 2016). Due to evaporation and limited flow, particularly during summer, salinity was constantly higher at this reef site. However, the difference to the other sites was miniscule and probably negligible as stressor to calcifying (Röthig et al., 2016) and bioeroding biota. The strong variability of diurnal pH on the other hand is supposedly influencing performance of calcifiers and bioeroders. Previously, small scale pH anomalies were demonstrated to correlate with net accretion dynamics by showing higher net accretion prevailing in sites of less variable pH conditions locally (Price et al., 2012; Silbiger et al., 2014), which reflects the pattern that we observe in our study. pH fluctuation is a biotic feedback signature in reef habitats, which entails changes in sea water chemistry caused by dominant biotic processes, i.e., calcification, carbonate dissolution, and respiration/photosynthesis (Bates et al., 2010; Silverman et al., 2007a; Zundelevich et al., 2007). This fluctuation accompanies changes in other factors such as carbonate system variables, e.g. pCO_2, aragonite saturation state (Shaw et al., 2012; Silbiger et al., 2014), which again can modify the antagonistic processes of calcification and bioerosion, i.e., dissolution (e.g., Andersson, 2015; Langdon et al., 2000; Tribollet et al., 2009).

At the first glance, the nearshore reef seems to be of little importance to the growth and maintenance of the reef framework due to its low carbonate productivity. Yet, such a less productive habitat can become critical to the resilience of the reef system. Reef biota, most importantly calcifiers, that reside under prevailing highly variable and presumably challenging conditions such as experienced at the nearshore reef are likely to be more stress resilient and survive under extreme events, e.g. heat waves (Camp et al., 2018; Rivest et al., 2017; Schoepf et al., 2015). This may benefit the resilience and recovery of organisms on a larger scale, for instance by functioning as a larval source. In particular, reef-building coral populations, which count as the most susceptible biota regarding climatic and human-made disturbance may benefit from such communities.

Total alkalinity and nutrients

The increase in TA is often associated with increased carbonate ion concentration and aragonite saturation state, which facilitate the precipitation of carbonates supporting the performance of reef-builders (Albright et al., 2016, 2018; Langdon et al., 2000; Schneider and Erez, 2006; Silbiger et al., 2014). We identified a positive correlation of TA with reef growth in our dataset. The difference in TA across our study sites was small, but in the range of a natural cross-shelf difference reported from other reefs (e.g. reefs in Bermuda, 20 - 40 µmol TA kg^{-1}, Bates et al., 2010), and as

high as 50 µmol kg^{-1}, the TA enrichment that enhanced net community calcification in a reef-enclosed lagoon (Albright et al., 2016). On the other hand, high calcification rates can deplete TA, whereas dissolution of carbonates can enrich TA measurably, specifically in (semi) enclosed systems (Bates et al., 2010), which we do not observe along the cross shelf gradient. It remains to be further investigated how TA dynamics across the shelf relate to reef growth processes.

Although increased nutrients are commonly linked to reef degradation initiated through phase-shift, increased bioerosion rates, and/or the decline of calcifiers (Fabricius, 2011; Grand and Fabricius, 2010; Holmes, 2000), our dataset suggests that a highly oligotrophic system such as the central Red Sea reefs may benefit from slight increases of certain nutrient species. Specifically, natural minor increases of N and P might have a positive effect on ecosystem productivity and functioning including carbonate budgets. A moderate natural source of nutrients, e.g., from sea bird populations, can indeed have a positive effect on ecosystem functioning, in contrast to anthropogenic run-off (Graham et al., 2018). Interestingly, our study also identified PO_4^{3-} concentration as an abiotic correlate of reef growth. In the Red Sea high N:P ratios indicate that P is a limiting micronutrient, e.g. for phytoplankton (Fahmy, 2003). PO_4^{3-} is not only essential for pelagic primary producers, but also for reef calcifiers and their photosymbionts, such as the stony corals and their micro-algal *Symbiodinium* endosymbionts (Ferrier-Pagès et al., 2016). Experimental studies have demonstrated that PO_4^{3-} provision can maintain the coral-algae symbiosis in reef-building corals under heat stress (Ezzat et al., 2016). Conversely, P limitation can increase the stress susceptibility of this symbiosis (Pogoreutz et al., 2017; Rädecker et al., 2015; Wiedenmann et al., 2013). In light of our results, it will be of interest to link spatio-temporal variation of inorganic nutrient ratios with patterns of reef resilience in the central Red Sea to understand their effects on long-term trends of reef growth.

4.4 Reef growth trajectories in the Red Sea

Carbonate budgets provide an insight into ecosystem functioning and can be used as a powerful tool to track reef trajectories through time. This includes the exploration of past and current reef trends, which may be critical for prediction of future reef development (Januchowski-Hartley et al., 2017). Indeed, the absence of comparative baseline data limits a historical perspective on the central Red Sea G_{budget} presented here. Previously reported Red Sea data include pelagic and reefal net carbonate accretion rates from 1998, estimated using basin-scale historical measurements of TA (Steiner et al., 2014). Another dataset employs the census-based budget approach for a highly seasonal high-latitude fringing reef in the Gulf of Aqaba (GoA) from 1994 - 1996 (Dullo et al., 1996), which is methodologically similar to the *ReefBudget* approach. Both reef growth estimates provide similar rates: The TA-based reef accretion estimate from 1998 was 0.9 kg $m^{-2}y^{-1}$ and the GoA fringing reef budget from 1994 - 1996 ranged between 0.7 and 0.9 kg $m^{-2}y^{-1}$. Additionally, the gross calcification rate of the offshore benthic communities ($G_{benthos}$) compares well with the maxima measured in GoA reefs in 1994 (i.e., 2.7 kg $m^{-2}y^{-1}$) (Heiss, 1995). The $G_{budgets}$ assessed in the present study are in accordance with these data, indicating stable reef growth rates in the Red Sea basin in the recent 20 years, despite the ongoing warming trend and observed impairment in coral calcification in a coral species (Cantin et al., 2010; Raitsos et al., 2011). Yet, data are limited and comparisons between the central Red Sea and GoA

should be interpreted with great caution. Due to the strong latitudinal gradient of temperature and salinity along with differences in seasonality between the central Red Sea and GoA, reef growth dynamics from the two regions may fundamentally differ and introduce bias. Hence, far larger (and ideally corss-latitude) datasets will be needed to determine more accurately whether a declining calcification capacity of Red Sea corals has already become a basin-scale phenomenon, and whether there are species-specific differences. In this study we have demonstrated that offshore reefs in the central Red Sea still maintain a positive carbonate budget, yet can still be considered 'underperforming' below "optimal reefal production" (Vecsei, 2004). Further, our data present a snapshot along one environmental gradient. In the future more study sites should be included to provide a more accurate representation of the region. Past trajectories of reef growth in the Red Sea could provide evidence whether the 'suboptimal' reef growth in the central Red Sea is a present-day phenomenon, or whether this observation constitutes a true baseline of reef growth in this naturally high temperature environment. It will be necessary to feed suitable historical census data into a carbonate budget approach (*sensu* Januchowski-Hartley et al. 2017), or apply a geological approach that makes use of fossil reef records to compare past and present reef growth processes. In the context of reef growth trajectories, the data presented in this study will serve as a valuable contemporary baseline for comparative future studies in the central Red Sea. Importantly, these data were collected before the Third Global Bleaching Event, which impacted the region during summer 2015 (Monroe et al., 2018) and 2016. The present effort therefore will be of great value when assessing potential (long-term) changes of Red Sea G_{budget} following this significant disturbance.

5 Conclusions

The Red Sea is a geographic region where coral reefs exist in a naturally high temperature and high salinity environment. Baseline data for reef growth from this region are particularly valuable as they provide insight into reef functioning that deviate from the global average for coral reefs, and can potentially provide an outlook to future ocean scenarios. The differences of central Red Sea reef growth dynamics to other major reef systems demonstrate the importance of *in situ* studies in underexplored major reef regions. For instance, our study highlights the importance of coralline algae as a reef-building agent in the region and shows that the erosive forces in the Red Sea are not as pronounced (yet) as observed elsewhere. Our data suggests that reef growth on Red Sea offshore reefs is comparable to the majority of reef growth estimates from other geographic regions, which today perform well below a 'healthy reef' carbonate budget. A first comparison with data from recent years suggests that reef growth rates in the central Red Sea might not have decreased substantially over the last two decades, despite potential negative effects of the ongoing warming trend. The absence of comparative long-term data from the region hampers predictions on long-term trajectories. We therefore advocate more detailed research to tackle past and future trajectories of reef growth dynamics under consideration of the challenging and unique environmental settings of the Red Sea.

Acknowledgements

We thank the Coastal and Marine Resources Lab (CMOR) at King Abdullah University of Science and Technology (KAUST) for logistics and operations at sea (E. Al-Jahdali, A. Al-Jahdali, G. Al-Jahdali, R. Al-Jahdali, H. Al-Jahdali, F. Mallon, P. Müller, and D. Pallett), as well as for the assistance with the deployment of oceanographic instruments

(L. Smith, M.D. Pantalita, and S. Mahmoud). We would like to acknowledge field assistance by C. Roder and C. Walcher in setting up the monitoring sites. We thank M. Khalil for providing a map of the study sites. Research reported in this publication was supported by funding to CRV from King Abdullah University of Science and Technology (KAUST).

Data availability.

Relevant data are available from the the manuscript and supplementary . In addition, physicochemical raw data is available from the Dryad Digital Repository *(will be included after review)*

Supplement link. The Supplementary material related to this article is available online *(will be included by Copernicus)*

Author contribution

Resources: CRV

Project administration: CRV

Conceptualization: AR

Investigation: AR TR CP

Methodology: AR TR CP

Formal analysis: AR CP VS

Validation: AR CP TR VS CRV

Visualization: AR

Funding acquisition: CRV

Writing - original draft: AR

Writing – review & editing: CRV TR CP VS AR

Data curation: AR

Competing interests

The authors declare that they have no conflict of interest.

References

Acker, J., Leptoukh, G., Shen, S., Zhu, T. and Kempler, S.: Remotely-sensed chlorophyll a observations of the northern Red Sea indicate seasonal variability and influence of coastal reefs, J. Mar. Syst., 69(3), 191–204, doi:10.1016/j.jmarsys.2005.12.006, 2008.

Albright, R., Caldeira, L., Hosfelt, J., Kwiatkowski, L., Maclaren, J. K., Mason, B. M., Nebuchina, Y., Ninokawa, A., Pongratz, J., Ricke, K. L., Rivlin, T., Schneider, K., Sesboüé, M., Shamberger, K., Silverman, J., Wolfe, K., Zhu, K. and Caldeira, K.: Reversal of ocean acidification enhances net coral reef calcification, Nature, advance online publication, doi:10.1038/nature17155, 2016.

Albright, R., Takeshita, Y., Koweek, D. A., Ninokawa, A., Wolfe, K., Rivlin, T., Nebuchina, Y., Young, J. and Caldeira, K.: Carbon dioxide addition to coral reef waters suppresses net community calcification, Nature, 555(7697), 516–519, doi:10.1038/nature25968, 2018.

677 Alwany, M. A., Thaler, E. and Stachowitsch, M.: Parrotfish bioerosion on Egyptian Red Sea reefs, J. Exp. Mar. Biol.
678 Ecol., 371(2), 170–176, doi:10.1016/j.jembe.2009.01.019, 2009.

679 Anderson, M. J., Gorley, R. N. and Clarke, K. R.: PERMANOVA+ for PRIMER: Guide to software and statistical
680 methods, 2008.

681 Andersson, A. J.: A Fundamental Paradigm for Coral Reef Carbonate Sediment Dissolution, Coral Reef Res., 2, 52,
682 doi:10.3389/fmars.2015.00052, 2015.

683 Bak, R. P. M.: Sea urchin bioerosion on coral reefs: place in the carbonate budget and relevant variables, Coral Reefs,
684 13(2), 99–103, doi:10.1007/BF00300768, 1994.

685 Bak, R. P. M., Nieuwland, G. and Meesters, E. H.: Coral Growth Rates Revisited after 31 Years: What is Causing
686 Lower Extension Rates in *Acropora Palmata*?, Bull. Mar. Sci., 84(3), 287–294, 2009.

687 Bannerot, S. P. and Bohnsack, J. A.: A stationary visual census technique for quantitatively assessing community
688 structure of coral reef fishes, NOAA. [online] Available from: http://core.kmi.open.ac.uk/download/pdf/11018492.pdf
689 (Accessed 1 September 2014), 1986.

690 Bates, N. R., Amat, A. and Andersson, A. J.: Feedbacks and responses of coral calcification on the Bermuda reef
691 system to seasonal changes in biological processes and ocean acidification, Biogeosciences, 7(8), 2509–2530,
692 doi:10.5194/bg-7-2509-2010, 2010.

693 Bellwood, D. R.: Direct estimate of bioerosion by two parrotfish species, *Chlorurus gibbus* and *C. sordidus*, on the
694 Great Barrier Reef, Australia, Mar. Biol., 121(3), 419–429, doi:10.1007/BF00349451, 1995.

695 Bellwood, D. R., Hoey, A. S. and Choat, J. H.: Limited functional redundancy in high diversity systems: resilience
696 and ecosystem function on coral reefs, Ecol. Lett., 6(4), 281–285, 2003.

697 Boyd, P. and Hutchins, D.: Understanding the responses of ocean biota to a complex matrix of cumulative
698 anthropogenic change, Mar. Ecol. Prog. Ser., 470, 125–135, doi:10.3354/meps10121, 2012.

699 Boyd, P. W. and Brown, C. J.: Modes of interactions between environmental drivers and marine biota, Front. Mar.
700 Sci., 2, doi:10.3389/fmars.2015.00009, 2015.

701 Browne, N. K., Smithers, S. G. and Perry, C. T.: Carbonate and terrigenous sediment budgets for two inshore turbid
702 reefs on the central Great Barrier Reef, Mar. Geol., 346, 101–123, doi:10.1016/j.margeo.2013.08.011, 2013.

703 Bruggemann, J., van Kessel, A., van Rooij, J. and Breeman, A.: Bioerosion and sediment ingestion by the Caribbean
704 parrotfish *Scarus vetula* and *Sparisoma viride*: implications of fish size, feeding mode and habitat use, Mar. Ecol.
705 Prog. Ser., 134, 59–71, doi:10.3354/meps134059, 1996.

706 Buddemeier, R. W.: Symbiosis: Making light work of adaptation, Nature, 388(6639), 229–230, doi:10.1038/40755,
707 1997.

708 Cai, W.-J., Ma, Y., Hopkinson, B. M., Grottoli, A. G., Warner, M. E., Ding, Q., Hu, X., Yuan, X., Schoepf, V., Xu,
709 H., Han, C., Melman, T. F., Hoadley, K. D., Pettay, D. T., Matsui, Y., Baumann, J. H., Levas, S., Ying, Y. and Wang,
710 Y.: Microelectrode characterization of coral daytime interior pH and carbonate chemistry, Nat. Commun., 7, 11144,
711 doi:10.1038/ncomms11144, 2016.

712 Camp, E. F., Nitschke, M. R., Rodolfo-Metalpa, R., Houlbreque, F., Gardner, S. G., Smith, D. J., Zampighi, M. and
713 Suggett, D. J.: Reef-building corals thrive within hot-acidified and deoxygenated waters, Sci. Rep., 7(1), 2434,
714 doi:10.1038/s41598-017-02383-y, 2017.

715 Camp, E. F., Schoepf, V., Mumby, P. J., Hardtke, L. A., Rodolfo-Metalpa, R., Smith, D. J. and Suggett, D. J.: The
716 Future of Coral Reefs Subject to Rapid Climate Change: Lessons from Natural Extreme Environments, Front. Mar.
717 Sci., 5, doi:10.3389/fmars.2018.00004, 2018.

718 Cantin, N. E., Cohen, A. L., Karnauskas, K. B., Tarrant, A. M. and McCorkle, D. C.: Ocean Warming Slows Coral
719 Growth in the Central Red Sea, Science, 329(5989), 322–325, doi:10.1126/science.1190182, 2010.

720 Carricart-Ganivet, J. P., Cabanillas-Terán, N., Cruz-Ortega, I. and Blanchon, P.: Sensitivity of Calcification to
721 Thermal Stress Varies among Genera of Massive Reef-Building Corals, PLoS ONE, 7(3), e32859,
722 doi:10.1371/journal.pone.0032859, 2012.

723 Chazottes, V., Campion-Alsumard, T. L. and Peyrot-Clausade, M.: Bioerosion rates on coral reefs: interactions
724 between macroborers, microborers and grazers (Moorea, French Polynesia), Palaeogeogr. Palaeoclimatol. Palaeoecol.,
725 113(2–4), 189–198, doi:10.1016/0031-0182(95)00043-L, 1995.

726 Chazottes, V., Le Campion-Alsumard, T., Peyrot-Clausade, M. and Cuet, P.: The effects of eutrophication-related
727 alterations to coral reef communities on agents and rates of bioerosion (Reunion Island, Indian Ocean), Coral Reefs,
728 21(4), 375–390, 2002.

729 Cohen, A. L. and Holcomb, M.: Why corals care about ocean acidification: uncovering the mechanism, Oceanography,
730 (22), 118–127, 2009.

731 Cooper, T. F., Death, G., Fabricius, K. E. and Lough, J. M.: Declining coral calcification in massive *Porites* in two
732 nearshore regions of the northern Great Barrier Reef, Glob. Change Biol., 14(3), 529–538, doi:10.1111/j.1365-
733 2486.2007.01520.x, 2008.

734 Couce, E., Ridgwell, A. and Hendy, E. J.: Environmental controls on the global distribution of shallow-water coral
735 reefs, J. Biogeogr., 39(8), 1508–1523, doi:10.1111/j.1365-2699.2012.02706.x, 2012.

736 Cyronak, T., Santos, I. R., McMahon, A. and Eyre, B. D.: Carbon cycling hysteresis in permeable carbonate sands
737 over a diel cycle: Implications for ocean acidification, Limnol. Oceanogr., 58(1), 131–143,
738 doi:10.4319/lo.2013.58.1.0131, 2013.

739 Death, G., Lough, J. M. and Fabricius, K. E.: Declining Coral Calcification on the Great Barrier Reef, Science,
740 323(5910), 116–119, doi:10.1126/science.1165283, 2009.

741 Dullo, P. D. W.-C., Gektidis, D. M., Golubic, P. D. S., Heiss, D. G. A., Kampmann, D. B. H., Kiene, D. W., Kroll, D.
742 Ö. D. K., Kuhrau, D. B. M. L., Radtke, D. G., Reijmer, D. J. G., Reinicke, D. G. B., Schlichter, P. D. D., Schuhmacher,
743 P. D. H. and Vogel, K.: Factors controlling holocene reef growth: An interdisciplinary approach, Facies, 32(1), 145–
744 188, doi:10.1007/BF02536867, 1995.

745 Dullo, W.-C., Reijmer, J., Schuhmacher, H., Eisenhauer, A., Hassan, M. and Heiss, G.: Holocene reef growth and
746 recent carbonate production in the Red Sea, [online] Available from:
747 https://www.researchgate.net/publication/230751439_Holocene_reef_growth_and_recent_carbonate_production_in
748 _the_Red_Sea, 1996.

749 Eakin, C. M.: A tale of two Enso Events: carbonate budgets and the influence of two warming disturbances and
750 intervening variability, Uva Island, Panama, Bull. Mar. Sci., 69(1), 171–186, 2001.

751 Edgar, G. J., Banks, S. A., Brandt, M., Bustamante, R. H., Chiriboga, A., Earle, S. A., Garske, L. E., Glynn, P. W.,
752 Grove, J. S., Henderson, S., Hickman, C. P., Miller, K. A., Rivera, F. and Wellington, G. M.: El Niño, grazers and
753 fisheries interact to greatly elevate extinction risk for Galapagos marine species, Glob. Change Biol., 16(10), 2876–
754 2890, doi:10.1111/j.1365-2486.2009.02117.x, 2010.

Edinger, E. N., Limmon, G. V., Jompa, J., Widjatmoko, W., Heikoop, J. M. and Risk, M. J.: Normal coral growth rates on dying reefs: Are coral growth rates good indicators of reef health?, Mar. Pollut. Bull., 40(5), 404–425, 2000.

Enochs, I. C.: Ocean acidification enhances the bioerosion of a common coral reef sponge: implications for the persistence of the Florida Reef Tract, Bull. Mar. Sci., 91, 271–290, doi:10.5343/bms.2014.1045, 2015.

Ezzat, L., Maguer, J.-F., Grover, R. and Ferrier-Pagès, C.: Limited phosphorus availability is the Achilles heel of tropical reef corals in a warming ocean, Sci. Rep., 6, 31768, doi:10.1038/srep31768, 2016.

Fabricius, K. E.: Factors Determining the Resilience of Coral Reefs to Eutrophication: A Review and Conceptual Model, in Coral Reefs: An Ecosystem in Transition, edited by Z. Dubinsky and N. Stambler, pp. 493–505, Springer Netherlands, Dordrecht. [online] Available from: http://www.springerlink.com/index/10.1007/978-94-007-0114-4_28 (Accessed 8 May 2012), 2011.

Fahmy, M.: Water quality in the Red Sea coastal waters (Egypt): Analysis of spatial and temporal variability, Chem. Ecol., 19(1), 67–77, doi:10.1080/0275754031000087074, 2003.

Fang, J. K. H., Mello-Athayde, M. A., Schönberg, C. H. L., Kline, D. I., Hoegh-Guldberg, O. and Dove, S.: Sponge biomass and bioerosion rates increase under ocean warming and acidification, Glob. Change Biol., 19(12), 3581–3591, doi:10.1111/gcb.12334, 2013.

Ferrier-Pagès, C., Godinot, C., D'Angelo, C., Wiedenmann, J. and Grover, R.: Phosphorus metabolism of reef organisms with algal symbionts, Ecol. Monogr., 86(3), 262–277, doi:10.1002/ecm.1217, 2016.

Franco, C., Hepburn, L. A., Smith, D. J., Nimrod, S. and Tucker, A.: A Bayesian Belief Network to assess rate of changes in coral reef ecosystems, Environ. Model. Softw., 80, 132–142, doi:10.1016/j.envsoft.2016.02.029, 2016.

Glynn, P. W.: Bioerosion and coral-reef growth: a dynamic balance, in Life and Death of Coral Reefs, edited by C. Birkeland, pp. 68–94, Chapman and Hall, Ney York, USA., 1997.

Glynn, P. W. and Manzello, D. P.: Bioerosion and Coral Reef Growth: A Dynamic Balance, in Coral Reefs in the Anthropocene, edited by C. Birkeland, pp. 67–97, Springer Netherlands., 2015.

Graham, N. A. J., Wilson, S. K., Carr, P., Hoey, A. S., Jennings, S. and MacNeil, M. A.: Seabirds enhance coral reef productivity and functioning in the absence of invasive rats, Nature, 559(7713), 250–253, doi:10.1038/s41586-018-0202-3, 2018.

Grand, H. M. L. and Fabricius, K. E.: Relationship of internal macrobioeroder densities in living massive Porites to turbidity and chlorophyll on the Australian Great Barrier Reef, Coral Reefs, 30(1), 97–107, doi:10.1007/s00338-010-0670-x, 2010.

Grange, J. S., Rybarczyk, H. and Tribollet, A.: The three steps of the carbonate biogenic dissolution process by microborers in coral reefs (New Caledonia), Environ. Sci. Pollut. Res., doi:10.1007/s11356-014-4069-z, 2015.

Green, A. L. and Bellwood, D. R.: Monitoring functional groups of herbivorous reef fishes as indicators of coral reef resilience: a practical guide for coral reef managers in the Asia Pacific region, International Union for Conservation of Nature, IUCN, Gland, Switzerland. [online] Available from: ftp://ftp.library.noaa.gov/noaa_documents.lib/CoRIS/IUCN_herbivorous_reef-fishes_2009.pdf (Accessed 30 September 2017), 2009.

Heiss, G. A.: Carbonate production by scleractinian corals at Aqaba, Gulf of Aqaba, Red Sea, Facies, 33(1), 19–34, doi:10.1007/BF02537443, 1995.

Heyward, A. J. and Negri, A. P.: Natural inducers for coral larval metamorphosis, Coral Reefs, 18(3), 273–279, 1999.

Hoey, A. S. and Bellwood, D. R.: Cross-shelf variation in the role of parrotfishes on the Great Barrier Reef, Coral Reefs, 27(1), 37–47, doi:10.1007/s00338-007-0287-x, 2007.

Holmes, K. E.: Effects of eutrophication on bioeroding sponge communities with the description of new West Indian sponges, *Cliona spp.* (Porifera: Hadromerida: Clionidae), Invertebr. Biol., 119(2), 125–138, doi:10.1111/j.1744-7410.2000.tb00001.x, 2000.

Hughes, T. P., Rodrigues, M. J., Bellwood, D. R., Ceccarelli, D., Hoegh-Guldberg, O., McCook, L., Moltschaniwskyj, N., Pratchett, M. S., Steneck, R. S. and Willis, B.: Phase Shifts, Herbivory, and the Resilience of Coral Reefs to Climate Change, Curr. Biol., 17(4), 360–365, doi:10.1016/j.cub.2006.12.049, 2007.

Hutchings, P. A.: Biological destruction of coral reefs, Coral Reefs, 4(4), 239–252, doi:10.1007/BF00298083, 1986.

Januchowski-Hartley, F. A., Graham, N. A. J., Wilson, S. K., Jennings, S. and Perry, C. T.: Drivers and predictions of coral reef carbonate budget trajectories, Proc R Soc B, 284(1847), 20162533, doi:10.1098/rspb.2016.2533, 2017.

Jokiel, P. L. and Coles, S. L.: Response of Hawaiian and other Indo-Pacific reef corals to elevated temperature, Coral Reefs, 8(4), 155–162, doi:10.1007/BF00265006, 1990.

Jones, N. S., Ridgwell, A. and Hendy, E. J.: Evaluation of coral reef carbonate production models at a global scale, Biogeosciences, 12(5), 1339–1356, doi:10.5194/bg-12-1339-2015, 2015.

Kattan, A., Coker, D. J. and Berumen, M. L.: Reef fish communities in the central Red Sea show evidence of asymmetrical fishing pressure, Mar. Biodivers., 1–12, doi:10.1007/s12526-017-0665-8, 2017.

Kennedy, E. V., Perry, C. T., Halloran, P. R., Iglesias-Prieto, R., Schönberg, C. H. L., Wisshak, M., Form, A. U., Carricart-Ganivet, J. P., Fine, M., Eakin, C. M. and Mumby, P. J.: Avoiding Coral Reef Functional Collapse Requires Local and Global Action, Curr. Biol., 23(10), 912–918, doi:10.1016/j.cub.2013.04.020, 2013.

Kleemann, K.: The Pectinid Bivalve Pedum spondy-loideum (Gmelin 1791): Amount of Surface and Volume Occupied in Host Corals From the Red Sea, Mar. Ecol., 22(1–2), 111–133, doi:10.1046/j.1439-0485.2001.01749.x, 2001.

Kleypas, J., Buddemeier, R. and Gattuso, J.-P.: The future of coral reefs in an age of global change, Int. J. Earth Sci., 90(2), 426–437, doi:10.1007/s005310000125, 2001.

Kleypas, J. A., McManus, J. W. and Menez, L. A. B.: Environmental Limits to Coral Reef Development: Where Do We Draw the Line?, Am. Zool., 39, 146–159, 1999.

Langdon, C., Takahashi, T., Sweeney, C., Chipman, D., Goddard, J., Marubini, F., Aceves, H., Barnett, H. and Atkinson, M. J.: Effect of calcium carbonate saturation state on the calcification rate of an experimental coral reef, Glob. Biogeochem. Cycles, 14(2), 639–654, doi:10.1029/1999GB001195, 2000.

Lazar, B. and Loya, Y.: Bioerosion of coral reefs - A chemical approach, Limnol. Oceanogr., 36, 377–383, 1991.

Manzello, D. P.: Ocean acidification hotspots: Spatiotemporal dynamics of the seawater CO_2 system of eastern Pacific coral reefs, Limnol. Oceanogr., 55(1), 239–248, doi:10.4319/lo.2010.55.1.0239, 2010.

Marshall, A. T. and Clode, P.: Calcification rate and the effect of temperature in a zooxanthellate and an azooxanthellate scleractinian reef coral, Coral Reefs, 23(2), 218–224, doi:10.1007/s00338-004-0369-y, 2004.

Marubini, F., Ferrier-Pagès, C., Furla, P. and Allemand, D.: Coral calcification responds to seawater acidification: a working hypothesis towards a physiological mechanism, Coral Reefs, 27(3), 491–499, doi:10.1007/s00338-008-0375-6, 2008.

McClanahan, T. R.: Kenyan coral reef lagoon fish: effects of fishing, substrate complexity, and sea urchins, Coral Reefs, 13(4), 231–241, doi:10.1007/BF00303637, 1994.

McClanahan, T. R. and Shafir, S. H.: Causes and consequences of sea urchin abundance and diversity in Kenyan coral reef lagoons, Oecologia, 83(3), 362–370, doi:10.1007/BF00317561, 1990.

McClanahan, T. R., Nugues, M. and Mwachireya, S.: Fish and sea urchin herbivory and competition in Kenyan coral reef lagoons: the role of reef management, J. Exp. Mar. Biol. Ecol., 184(2), 237–254, doi:10.1016/0022-0981(94)90007-8, 1994.

Metzl, N., Moore, B., Papaud, A. and Poisson, A.: Transport and carbon exchanges in Red Sea Inverse Methodology, Glob. Biogeochem. Cycles, 3(1), 1–26, doi:10.1029/GB003i001p00001, 1989.

Moberg, F. and Folke, C.: Ecological goods and services of coral reef ecosystems, Ecol. Econ., 29, 215–233, 1999.

Mokady, O., Lazar, B. and Loya, Y.: Echinoid bioerosion as a major structuring force of Red Sea coral reefs, Biol. Bull., 190(3), 367–372, 1996.

Monroe, A. A., Ziegler, M., Roik, A., Röthig, T., Hardenstine, R. S., Emms, M. A., Jensen, T., Voolstra, C. R. and Berumen, M. L.: *In situ* observations of coral bleaching in the central Saudi Arabian Red Sea during the 2015/2016 global coral bleaching event, PLoS ONE, 13(4), e0195814, doi:10.1371/journal.pone.0195814, 2018.

Mumby, P. J.: Herbivory versus corallivory: are parrotfish good or bad for Caribbean coral reefs?, Coral Reefs, 28(3), 683–690, doi:10.1007/s00338-009-0501-0, 2009.

Mumby, P. J. and Harborne, A. R.: Marine Reserves Enhance the Recovery of Corals on Caribbean Reefs, PLoS OEE, 5(1), e8657, doi:10.1371/journal.pone.0008657, 2010.

Orr, J. C., Fabry, V. J., Aumont, O., Bopp, L., Doney, S. C., Feely, R. A., Gnanadesikan, A., Gruber, N., Ishida, A., Joos, F., Key, R. M., Lindsay, K., Maier-Reimer, E., Matear, R., Monfray, P., Mouchet, A., Najjar, R. G., Plattner, G.-K., Rodgers, K. B., Sabine, C. L., Sarmiento, J. L., Schlitzer, R., Slater, R. D., Totterdell, I. J., Weirig, M.-F., Yamanaka, Y. and Yool, A.: Anthropogenic ocean acidification over the twenty-first century and its impact on calcifying organisms, Nature, 437(7059), 681–686, doi:10.1038/nature04095, 2005.

Osorno, A., Peyrot-Clausade, M. and Hutchings, P. A.: Patterns and rates of erosion in dead *Porites* across the Great Barrier Reef (Australia) after 2 years and 4 years of exposure, Coral Reefs, 24(2), 292–303, doi:10.1007/s00338-005-0478-2, 2005.

Pari, N., Peyrot-Clausade, M., Le Champion-Alsumard, T., Hutchings, P., Chazottes, V., Gobulic, S., Le Champion, J. and Fontaine, M. F.: Bioerosion of experimental substrates on high islands and on atoll lagoons (French Polynesia) after two years of exposure, Mar. Ecol. Prog. Ser., 166, 119–130, 1998.

Perry, C., Edinger, E., Kench, P., Murphy, G., Smithers, S., Steneck, R. and Mumby, P.: Estimating rates of biologically driven coral reef framework production and erosion: a new census-based carbonate budget methodology and applications to the reefs of Bonaire, Coral Reefs, 31(3), 853–868, doi:10.1007/s00338-012-0901-4, 2012.

Perry, C. T. and Morgan, K. M.: Bleaching drives collapse in reef carbonate budgets and reef growth potential on southern Maldives reefs, Sci. Rep., 7, 40581, doi:10.1038/srep40581, 2017.

Perry, C. T., Spencer, T. and Kench, P. S.: Carbonate budgets and reef production states: a geomorphic perspective on the ecological phase-shift concept, Coral Reefs, 27(4), 853–866, doi:10.1007/s00338-008-0418-z, 2008.

Perry, C. T., Murphy, G. N., Kench, P. S., Smithers, S. G., Edinger, E. N., Steneck, R. S. and Mumby, P. J.: Caribbean-wide decline in carbonate production threatens coral reef growth, Nat. Commun., 4, 1402, doi:10.1038/ncomms2409, 2013.

Perry, C. T., Murphy, G. N., Kench, P. S., Edinger, E. N., Smithers, S. G., Steneck, R. S. and Mumby, P. J.: Changing dynamics of Caribbean reef carbonate budgets: emergence of reef bioeroders as critical controls on present and future reef growth potential, Proc. R. Soc. B Biol. Sci., 281(1796), 20142018–20142018, doi:10.1098/rspb.2014.2018, 2014.

Perry, C. T., Murphy, G. N., Graham, N. A. J., Wilson, S. K., Januchowski-Hartley, F. A. and East, H. K.: Remote coral reefs can sustain high growth potential and may match future sea-level trends, Sci. Rep., 5, 18289, doi:10.1038/srep18289, 2015.

Perry, C. T., Morgan, K. M. and Yarlett, R. T.: Reef Habitat Type and Spatial Extent as Interacting Controls on Platform-Scale Carbonate Budgets, Front. Mar. Sci., 4, doi:10.3389/fmars.2017.00185, 2017.

Perry, C. T., Alvarez-Filip, L., Graham, N. A. J., Mumby, P. J., Wilson, S. K., Kench, P. S., Manzello, D. P., Morgan, K. M., Slangen, A. B. A., Thomson, D. P., Januchowski-Hartley, F., Smithers, S. G., Steneck, R. S., Carlton, R., Edinger, E. N., Enochs, I. C., Estrada-Saldívar, N., Haywood, M. D. E., Kolodziej, G., Murphy, G. N., Pérez-Cervantes, E., Suchley, A., Valentino, L., Boenish, R., Wilson, M. and Macdonald, C.: Loss of coral reef growth capacity to track future increases in sea level, Nature, 1, doi:10.1038/s41586-018-0194-z, 2018.

Pisapia, C., Burn, D., Yoosuf, R., Najeeb, A., Anderson, K. D. and Pratchett, M. S.: Coral recovery in the central Maldives archipelago since the last major mass-bleaching, in 1998, Sci. Rep., 6, 34720, doi:10.1038/srep34720, 2016.

Pogoreutz, C., Rädecker, N., Cárdenas, A., Gärdes, A., Voolstra, C. R. and Wild, C.: Sugar enrichment provides evidence for a role of nitrogen fixation in coral bleaching, Glob. Change Biol., 8, 23:3838–3848, doi:10.1111/gcb.13695, 2017.

Price, N. N., Martz, T. R., Brainard, R. E. and Smith, J. E.: Diel Variability in Seawater pH Relates to Calcification and Benthic Community Structure on Coral Reefs, PLoS ONE, 7(8), e43843, doi:10.1371/journal.pone.0043843, 2012.

R Core Team: R: A language and environment for statistical computing, R Foundation for Statistical Computing, Vienna, Austria. [online] Available from: http://www.R-project.org/, 2013.

Rädecker, N., Pogoreutz, C., Voolstra, C. R., Wiedenmann, J. and Wild, C.: Nitrogen cycling in corals: the key to understanding holobiont functioning?, Trends Microbiol., doi:10.1016/j.tim.2015.03.008, 2015.

Raitsos, D. E., Hoteit, I., Prihartato, P. K., Chronis, T., Triantafyllou, G. and Abualnaja, Y.: Abrupt warming of the Red Sea, Geophys. Res. Lett., 38(14), L14601, doi:10.1029/2011GL047984, 2011.

Reaka-Kudla, M., Feingold, J. and Glynn, W.: Experimental studies of rapid bioerosion of coral reefs in the Galapagos Islands, Coral Reefs, 15(2), 101–107, 1996.

Reaka-Kudla, M. L.: The Global Biodiversity of Coral Reefs: A Comparison with Rainforests, in Biodiversity II: Understanding and Protecting Our Biological Resources, edited by M. L. Reaka-Kudla, D. E. Wilson, and E. O. Wilson, pp. 83–106, The Joseph Henry Press, USA., 1997.

Riegl, B.: Climate change and coral reefs: different effects in two high-latitude areas (Arabian Gulf, South Africa), Coral Reefs, 22(4), 433–446, doi:10.1007/s00338-003-0335-0, 2003.

Riegl, B. M., Bruckner, A. W., Rowlands, G. P., Purkis, S. J. and Renaud, P.: Red Sea Coral Reef Trajectories over 2 Decades Suggest Increasing Community Homogenization and Decline in Coral Size, PLoS ONE, 7(5), e38396, doi:10.1371/journal.pone.0038396, 2012.

Rivest, E. B., Comeau, S. and Cornwall, C. E.: The Role of Natural Variability in Shaping the Response of Coral Reef Organisms to Climate Change, Curr. Clim. Change Rep., 3(4), 271–281, doi:10.1007/s40641-017-0082-x, 2017.

Roik, A., Roder, C., Röthig, T. and Voolstra, C. R.: Spatial and seasonal reef calcification in corals and calcareous crusts in the central Red Sea, Coral Reefs, 1–13, doi:10.1007/s00338-015-1383-y, 2015.

Roik, A., Röthig, T., Roder, C., Ziegler, M., Kremb, S. G. and Voolstra, C. R.: Year-Long Monitoring of Physico-Chemical and Biological Variables Provide a Comparative Baseline of Coral Reef Functioning in the Central Red Sea, PLoS ONE, 11(11), e0163939, doi:10.1371/journal. pone.0163939, 2016.

Röthig, T., Ochsenkühn, M. A., Roik, A., van der Merwe, R. and Voolstra, C. R.: Long-term salinity tolerance is accompanied by major restructuring of the coral bacterial microbiome, Mol. Ecol., 25(6), 1308–1323, doi:10.1111/mec.13567, 2016.

Sawall, Y. and Al-Sofyani, A.: Biology of Red Sea Corals: Metabolism, Reproduction, Acclimatization, and Adaptation, in The Red Sea, edited by N. M. A. Rasul and I. C. F. Stewart, pp. 487–509, Springer Berlin Heidelberg. [online] Available from: http://link.springer.com/chapter/10.1007/978-3-662-45201-1_28 (Accessed 7 April 2015), 2015.

Sawall, Y., Al-Sofyani, A., Hohn, S., Banguera-Hinestroza, E., Voolstra, C. R. and Wahl, M.: Extensive phenotypic plasticity of a Red Sea coral over a strong latitudinal temperature gradient suggests limited acclimatization potential to warming, Sci. Rep., 5, 8940, doi:10.1038/srep08940, 2015.

Schmidt, G. M. and Richter, C.: Coral Growth and Bioerosion of *Porites lutea* in Response to Large Amplitude Internal Waves, PLoS ONE, 8(12), e73236, doi:10.1371/journal.pone.0073236, 2013.

Schneider, K. and Erez, J.: The effect of carbonate chemistry on calcification and photosynthesis in the hermatypic coral *Acropora eurystoma*, Limnol. Oceanogr., 51(3), 1284–1293, 2006.

Schoepf, V., Stat, M., Falter, J. L. and McCulloch, M. T.: Limits to the thermal tolerance of corals adapted to a highly fluctuating, naturally extreme temperature environment, Sci. Rep., 5, 17639, doi:10.1038/srep17639, 2015.

Schönberg, C. H. L., Fang, J. K. H., Carreiro-Silva, M., Tribollet, A. and Wisshak, M.: Bioerosion: the other ocean acidification problem, ICES J. Mar. Sci., 74(4), 895–925, doi:10.1093/icesjms/fsw254, 2017.

Schuhmacher, H., Loch, K., Loch, W. and See, W. R.: The aftermath of coral bleaching on a Maldivian reef—a quantitative study, Facies, 51(1–4), 80–92, doi:10.1007/s10347-005-0020-6, 2005.

Shamberger, K. E. F., Lentz, S. J. and Cohen, A. L.: Low and variable ecosystem calcification in a coral reef lagoon under natural acidification, Limnol. Oceanogr., doi:10.1002/lno.10662, 2017.

Shaw, E. C., McNeil, B. I. and Tilbrook, B.: Impacts of ocean acidification in naturally variable coral reef flat ecosystems, J. Geophys. Res. Oceans, 117(C3), n/a–n/a, doi:10.1029/2011JC007655, 2012.

Sheppard, C. and Loughland, R.: Coral mortality and recovery in response to increasing temperature in the southern Arabian Gulf, Aquat. Ecosyst. Health Manag., 5(4), 395–402, doi:10.1080/14634980290002020, 2002.

Silbiger, N. J., Guadayol, O., Thomas, F. I. M. and Donahue, M. J.: Reefs shift from net accretion to net erosion along a natural environmental gradient, Mar. Ecol. Prog. Ser., 515, 33–44, doi:10.3354/meps10999, 2014.

Silverman, J., Lazar, B. and Erez, J.: Community metabolism of a coral reef exposed to naturally varying dissolved inorganic nutrient loads, Biogeochemistry, 84(1), 67–82, doi:10.1007/s10533-007-9075-5, 2007.

Steiner, Z., Erez, J., Shemesh, A., Yam, R., Katz, A. and Lazar, B.: Basin-scale estimates of pelagic and coral reef calcification in the Red Sea and Western Indian Ocean, Proc. Natl. Acad. Sci., 1414323111, doi:10.1073/pnas.1414323111, 2014.

949 Strahl, J., Stolz, I., Uthicke, S., Vogel, N., Noonan, S. H. C. and Fabricius, K. E.: Physiological and ecological
950 performance differs in four coral taxa at a volcanic carbon dioxide seep, Comp. Biochem. Physiol. A. Mol. Integr.
951 Physiol., 184, 179–186, doi:10.1016/j.cbpa.2015.02.018, 2015.

952 Tambutté, S., Holcomb, M., Ferrier-Pagès, C., Reynaud, S., Tambutté, É., Zoccola, D. and Allemand, D.: Coral
953 biomineralization: From the gene to the environment, J. Exp. Mar. Biol. Ecol., 408(1–2), 58–78,
954 doi:10.1016/j.jembe.2011.07.026, 2011.

955 Tribollet, A. and Golubic, S.: Cross-shelf differences in the pattern and pace of bioerosion of experimental carbonate
956 substrates exposed for 3 years on the northern Great Barrier Reef, Australia, Coral Reefs, 24(3), 422–434,
957 doi:10.1007/s00338-005-0003-7, 2005.

958 Tribollet, A. and Golubic, S.: Reef Bioerosion: Agents and Processes, in Coral Reefs: An Ecosystem in Transition,
959 edited by Z. Dubinsky and N. Stambler, pp. 435–449, Springer Netherlands, Dordrecht. [online] Available from:
960 http://www.springerlink.com/index/10.1007/978-94-007-0114-4_25 (Accessed 7 August 2012), 2011.

961 Tribollet, A., Decherf, G., Hutchings, P. and Peyrot-Clausade, M.: Large-scale spatial variability in bioerosion of
962 experimental coral substrates on the Great Barrier Reef (Australia): importance of microborers, Coral Reefs, 21(4),
963 424–432, doi:10.1007/s00338-002-0267-0, 2002.

964 Tribollet, A., Godinot, C., Atkinson, M. and Langdon, C.: Effects of elevated pCO_2 on dissolution of coral carbonates
965 by microbial euendoliths, Glob. Biogeochem. Cycles, 23(3), doi:10.1029/2008GB003286, 2009.

966 Uthicke, S., Doyle, J., Duggan, S., Yasuda, N. and McKinnon, A. D.: Outbreak of coral-eating Crown-of-Thorns
967 creates continuous cloud of larvae over 320 km of the Great Barrier Reef, Sci. Rep., 5, doi:10.1038/srep16885, 2015.

968 Vásquez-Elizondo, R. M. and Enríquez, S.: Coralline algal physiology is more adversely affected by elevated
969 temperature than reduced pH, Sci. Rep., 6, 19030, doi:10.1038/srep19030, 2016.

970 Vecsei, A.: A new estimate of global reefal carbonate production including the fore-reefs, Glob. Planet. Change, 43(1–
971 2), 1–18, doi:10.1016/j.gloplacha.2003.12.002, 2004.

972 Waldbusser, G. G., Hales, B. and Haley, B. A.: Calcium carbonate saturation state: on myths and this or that stories,
973 ICES J. Mar. Sci. J. Cons., 73(3), 563–568, doi:10.1093/icesjms/fsv174, 2016.

974 Wickham, H. and Chang, W.: ggplot2: An Implementation of the Grammar of Graphics. [online] Available from:
975 http://cran.r-project.org/web/packages/ggplot2/index.html (Accessed 25 June 2015), 2015.

976 Wiedenmann, J., D'Angelo, C., Smith, E. G., Hunt, A. N., Legiret, F.-E., Postle, A. D. and Achterberg, E. P.: Nutrient
977 enrichment can increase the susceptibility of reef corals to bleaching, Nat. Clim. Change, 3(2), 160–164,
978 doi:10.1038/nclimate1661, 2013.

979 Zaneveld, J. R., Burkepile, D. E., Shantz, A. A., Pritchard, C. E., McMinds, R., Payet, J. P., Welsh, R., Correa, A. M.
980 S., Lemoine, N. P., Rosales, S., Fuchs, C., Maynard, J. A. and Thurber, R. V.: Overfishing and nutrient pollution
981 interact with temperature to disrupt coral reefs down to microbial scales, Nat. Commun., 7, 11833,
982 doi:10.1038/ncomms11833, 2016.

983 Zundelevich, A., Lazar, B. and Ilan, M.: Chemical versus mechanical bioerosion of coral reefs by boring sponges -
984 lessons from Pione cf. vastifica, J. Exp. Biol., 210(1), 91–96, doi:10.1242/jeb.02627, 2007.

985

Figures

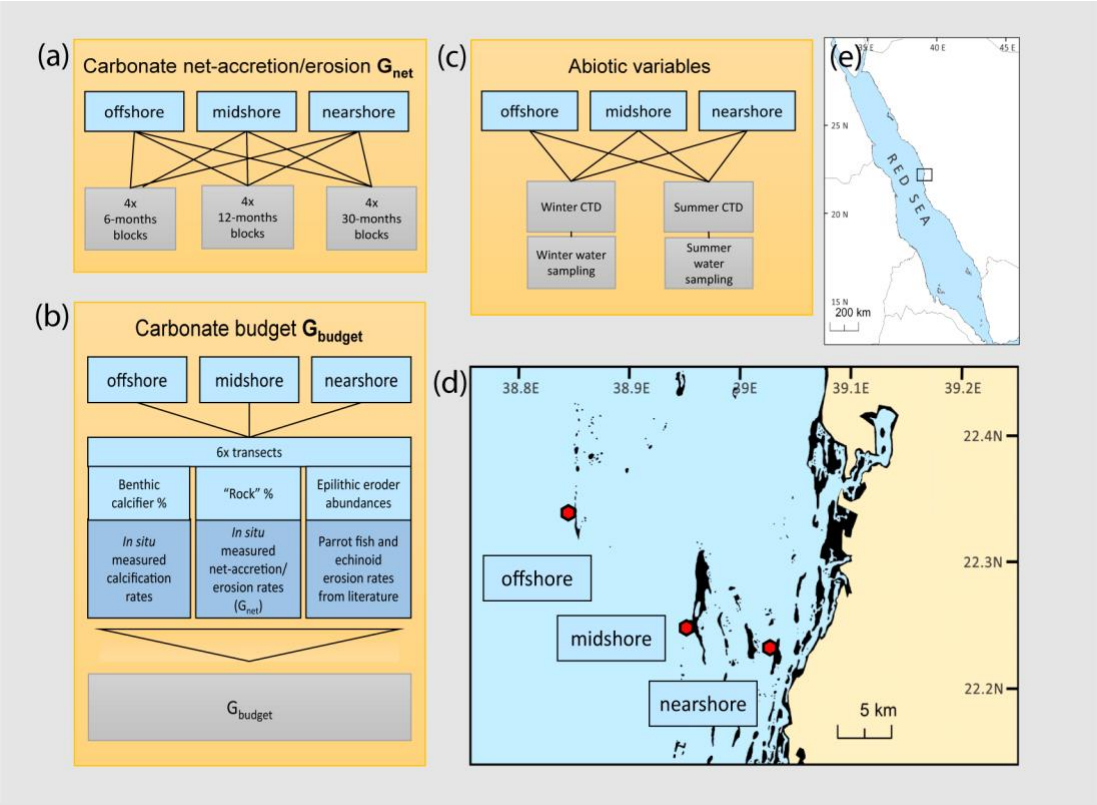

Figure 1. Design of studies and reef sites in the central Red Sea. Schemes in (a) – (c) summarize the study designs for the assessment of the two reef growth metric, G_{net} and G_{budget}, and the characterization of the abiotic environments in the central Red Sea. Maps (d) – (e) indicate geographic location and the study sites along a cross-shelf gradient. (Maps have been adapted from Roik et al. (2015); map credits: Maha Khalil).

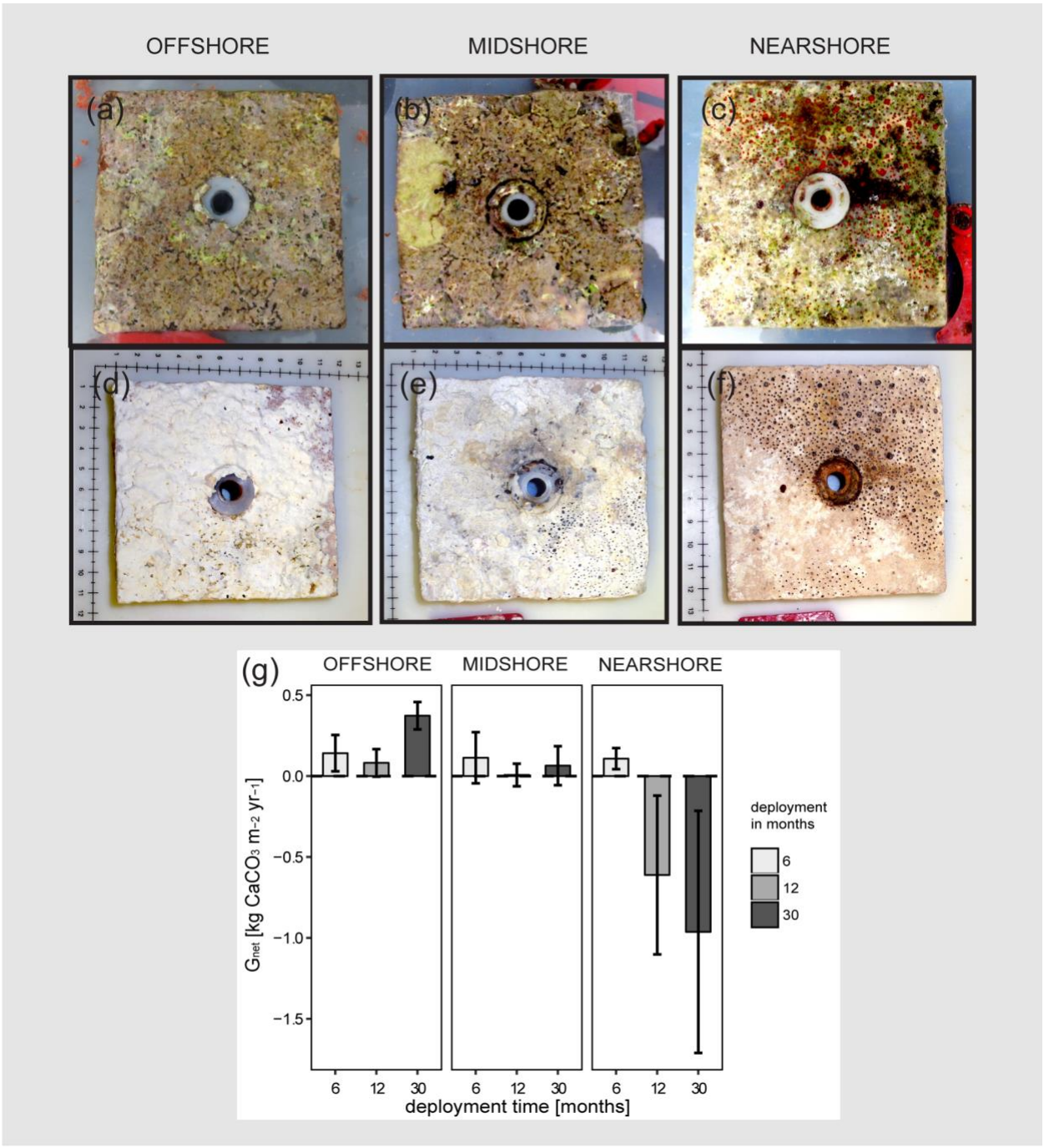

Figure 2. Net-accretion/-erosion rates (G_{net}) in the central Red Sea. G_{net} were measured *in situ* using limestone blocks (100 x 100 mm) that were deployed in the reefs, each set of blocks for 6, 12, or 30 months. Photos (a), (b), and (c), show freshly collected limestone blocks that were recovered after the deployment for 30 months. In the photos (d), (e), and (f) the same blocks after bleaching and drying are presented. Boring holes of endolithic sponges are clearly visible in blocks from the nearshore and midshore reef sites. Blocks from the midshore and offshore reefs were covered with crusts of biogenic carbonate mostly accreted by coralline algae assemblages (scales in the photos show cm). G_{net} data obtained from the limestone block assay are plotted in (g). All data are presented as mean ± standard deviation.

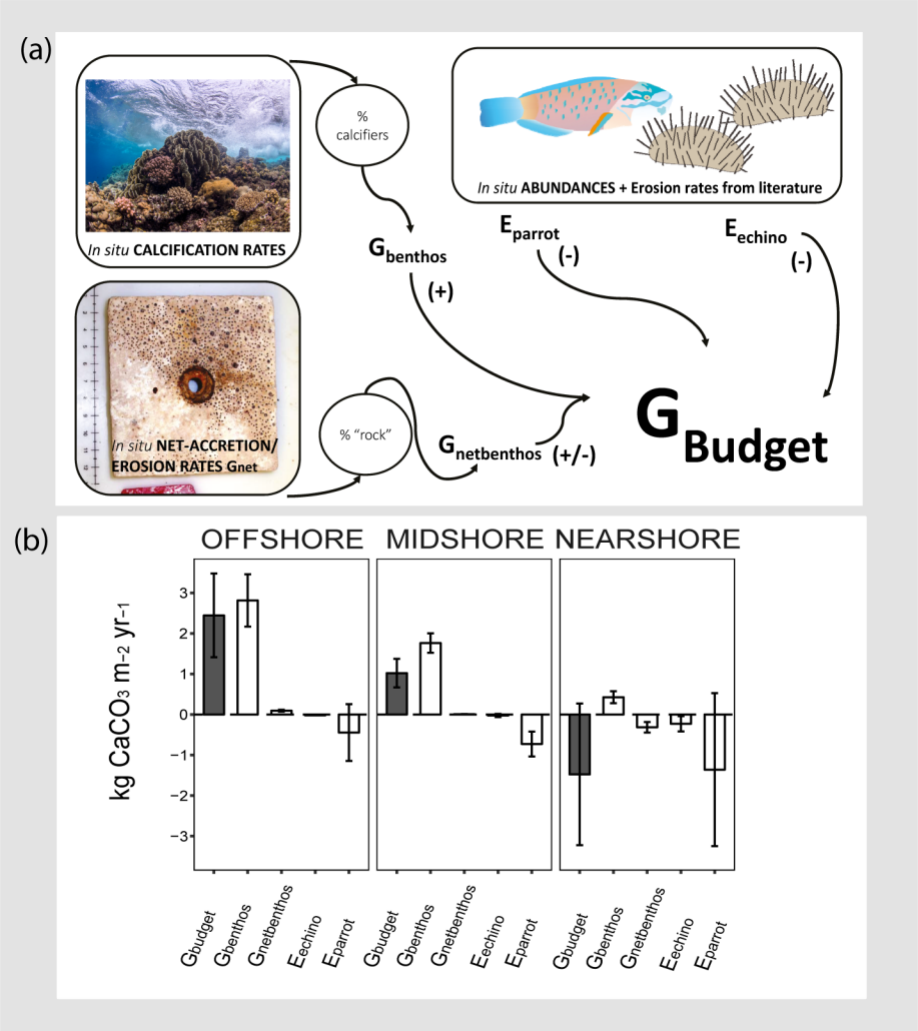

Figure 3. Census-based carbonate budgets in the central Red Sea. A schematic overview of the census-based carbonate budget approach that follows the *ReefBudget* approach adapted from Perry et al., (2012) is displayed in (a). Details on input data and equations, employed in the calculations, are available as Supplementary Materials (Text S1 and respective Supplemental tables). In (b) reef carbonate budgets are plotted in dark grey (G_{budget}) and related biotic variables in white. The biotic variables, i.e., site-specific calcification rates of benthic communities (**$G_{benthos}$**), net-accretion/-erosion rates of reef "rock" surface area ($G_{netbenthos}$), and the epilithic erosion rates of echinoids and parrotfishes (E_{echino}, E_{parrot}) contribute to the total reef carbonate budget (G_{budget}) at each reef site. Images from www.ian.umces.edu; photos by A.Roik. All data are presented as mean ± standard deviation.

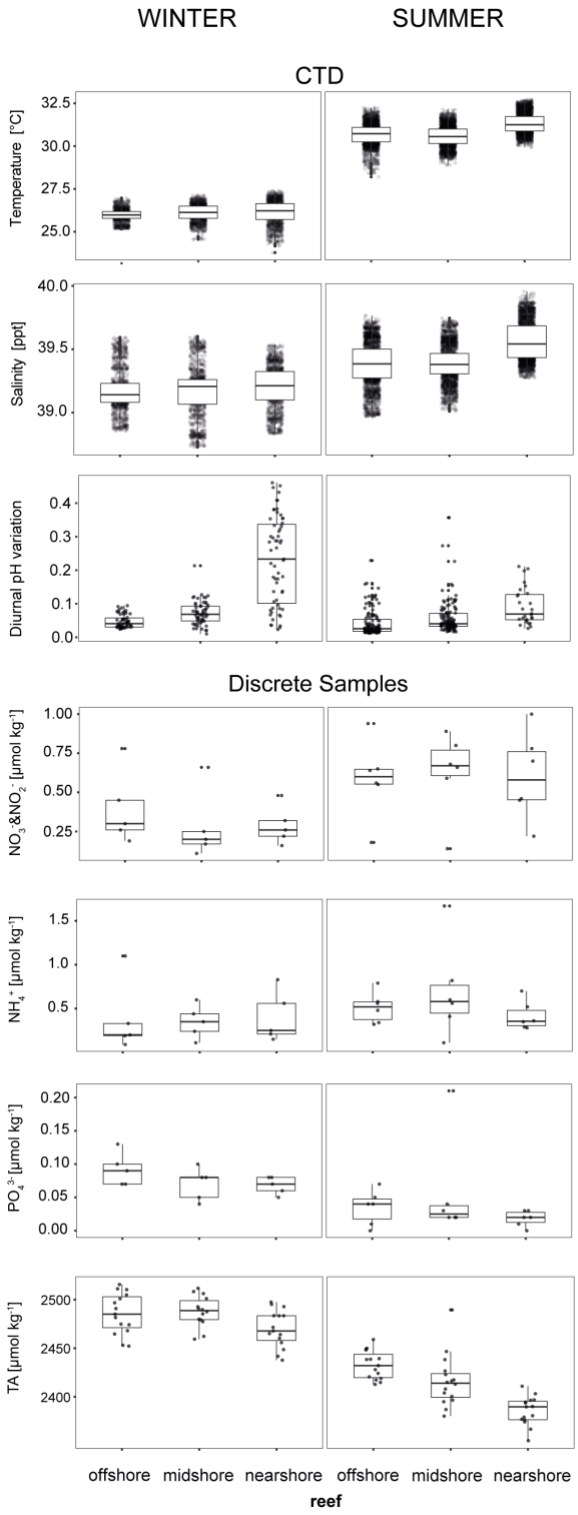

Figure 4. Abiotic conditions in the reef sites. Temperature, salinity, and diurnal pH_{NBS} variation (= diurnal standard deviations) were measured continuously over the respective seasons by CTDs (conductivity-temperature-depth loggers including an auxiliary pH probe). Furthermore, inorganic nutrients and total alkalinity (TA) were measured in discrete samples across reef sites and seasons. Boxplots illustrate the differences of seawater parameters between the reefs within each season (box: 1st and 3rd quartiles, whiskers: 1.5-fold inter-quartile range, points: raw data scatter).

Tables

Table 1. Glossary of reef growth metrics

Metric	Description	Input data for calculation of the metric
G_{net}	Site-specific net-accretion/-erosion rates (internal and epilithic) measured *in situ* using limestone blocks	-
***G_{budget}**	Ecosystem-scale census-based carbonate budget of a reef site	$G_{benthos}$, $G_{netbenthos}$, $G_{netbenthos}$, E_{echino}, E_{parrot}
$G_{benthos}$	Census-based calcification rate of benthic calcifier community (corals and coralline algae) per reef site	Site-specific benthic calcification rates (collated from this study and from Roik et al. 2015)
$G_{netbenthos}$	Census-based net-accretion/-erosion rates of reef "rock" surface area per reef site	Site-specific net-accretion/-erosion rates measured in this study using limestone blocks (G_{net})
E_{echino}	Census-based echinoid (sea urchin) erosion rates per reef site	Genus and size specific erosion rates for sea urchins from literature
E_{parrot}	Census-based parrotfish erosion rate per reef site	Genus and size specific erosion rates for parrotfishes from literature

*The method of G_{budget} calculation is described in the supplements (please refer to Text S1)

Table 2. Net-accretion/-erosion rates G_{net} in coral reefs along a cross-shelf gradient in the central Red Sea. G_{net} [kg m^{-2} y^{-1}] was calculated using weight gain/loss of limestone blocks that were deployed in the reefs. For each deployment duration, 6, 12, and 30 months, a set of 4 replicate blocks was used. Each block was measured once. Means per reef site and standard deviations in brackets; y = year

G_{net} [kg m^{-2} y^{-1}]	Deployment time [months]		
Reef site	**6**	**12**	**30**
Offshore	0.14(0.11)	0.08(0.09)	0.37(0.08)
Midshore	0.11(0.16)	0.01(0.07)	0.06(0.12)
Nearshore	0.11(0.07)	-0.61(0.49)	-0.96(0.75)

Table 3. Reef carbonate budgets and contributing biotic variables [kg m^{-2} y^{-1}] along a cross-shelf gradient in the central Red Sea. Calcification rates of benthic calcifiers **(**$G_{benthos}$), net-accretion/-erosion rates of the reef "rock" surface area ($G_{netbenthos}$), and the erosion rates of echinoids and parrotfishes (E_{echino}, E_{parrot}) contribute to the total carbonate budget (G_{budget}) in a reef site. Means per site are shown and standard deviations are in brackets.

Reef	G_{budget}	$G_{benthos}$	$G_{netbenthos}$	E_{echino}	E_{parrot}
Offshore	2.44(1.03)	2.81(0.65)	0.09(0.02)	-0.02(0)	-0.44(0.7)
Midshore	1.02(0.35)	1.76(0.24)	0.01(0)	-0.02(0.04)	-0.73(0.31)
Nearshore	-1.48(1.75)	0.43(0.15)	-0.31(0.13)	-0.23(0.19)	-1.36(1.89)

Table 4. Abiotic parameters relevant for reef growth at the study sites along a cross-shelf gradient in the central Red Sea. Temperature (Temp), salinity (Sal), and diurnal pH variation (diurnal SDs of pH_{NBS} measurements) were continuously measured using *in situ* probes (CTDs). Weekly collected seawater samples were used for the determination of inorganic nutrient concentrations, i.e. nitrate and nitrite (NO_3^-&NO_2^-), ammonia (NH_4^+), phosphate (PO_4^{3-}), and total alkalinity (TA). Mean (standard deviation).

Site / Season	**Temp**	**Sal**	**Diurnal pH variation**	**NO_3^- &NO_2^-**	**NH_4^+**	**PO_4^{3-}**	**TA**
	[°C]	**[ppt]**		**[µmol kg^{-1}]**	**[µmol kg^{-1}]**	**[µmol kg^{-1}]**	**[µmol kg^{-1}]**
Avg. winter	26.07(0.54)	39.18(0.18)	0.11(0.12)	0.32(0.19)	0.38(0.29)	0.08(0.02)	2487(20)
Avg. summer	30.85(0.69)	39.44(0.18)	0.05(0.05)	0.61(0.25)	0.54(0.34)	0.04(0.05)	2417(27)
Nearshore / winter	26.13(0.69)	39.2(0.17)	0.23(0.14)	0.29(0.12)	0.4(0.29)	0.07(0.01)	2476(19)
Nearshore / summer	31.32(0.59)	39.56(0.15)	0.09(0.06)	0.6(0.28)	0.42(0.16)	0.02(0.01)	2391(15)
Midshore / winter	26.1(0.49)	39.17(0.2)	0.07(0.04)	0.28(0.22)	0.35(0.19)	0.07(0.02)	2494(16)
Midshore / summer	30.56(0.61)	39.39(0.14)	0.05(0.05)	0.63(0.26)	0.7(0.53)	0.06(0.08)	2422(26)
Offshore / winter	25.97(0.36)	39.18(0.16)	0.04(0.02)	0.4(0.23)	0.38(0.41)	0.09(0.02)	2492(21)
Offshore / summer	30.68(0.63)	39.38(0.17)	0.04(0.04)	0.59(0.24)	0.51(0.17)	0.04(0.03)	2439(15)

Table 5. Coefficients from Spearman rank order correlations for abiotic and biotic predictor variables vs. G_{net} and G_{budget}. The means abiotic and biotic variables per reef site were correlated with G_{net} (= net-accretion/-erosion rates of limestone blocks) and G_{budget} (= census-based carbonate budgets). Strong and significant correlations (ρ values > |0.75|) are marked in **bold**. *P*-values were adjusted by the Benjamini-Hochberg method. CCA = crustose coralline algae; CC = calcifying crusts

	G_{net}		G_{budget}	
Abiotic variables	**ρ**	***p*(adj.)**	**ρ**	***p*(adj.)**
Temperature	-0.47	*n.s.*	-0.52	*n.s*
Salinity	**-0.82**	*< 0.01*	**-0.82**	*0.001*
Diurnal pH variation	**-0.95**	*< 0.001*	**-0.89**	*< 0.001*
NO_3^-&NO_2^-	**0.95**	*< 0.001*	**0.89**	*< 0.001*
NH_4^+	0.47	*n.s.*	0.52	*n.s.*
PO_4^{3-}	**0.82**	*< 0.01*	**0.82**	*0.001*
TA	**0.95**	*< 0.001*	**0.89**	*< 0.001*
Biotic variables	**ρ**	***p*(adj.)**	**ρ**	***p*(adj.)**
% cover CCA/CC	**0.95**	*< 0.001*	**0.78**	*< 0.01*
% cover Algae/Soft coral/Sponge	0.47	*n.s.*	0.26	*n.s.*
Parrot fish abundance	**-0.95**	*< 0.001*	-0.49	*n.s.*
Echinoid abundance	0.47	n.s.	-0.54	*n.s.*
% cover branching hard corals			-0.25	*n.s.*
% cover encrusting hard corals			0.26	*n.s.*
% cover massive hard corals			0.34	*n.s.*
% cover foliose hard corals			0.50	*n.s.*
% cover Acroporidae			0.27	*n.s.*
% cover Pocilloporidae			0.51	*n.s.*
% cover Poritidae			0.45	*n.s.*
% cover hard coral			0.63	*n.s.*
Rugosity			**0.75**	*< 0.01*